Cape Peninsula
University of Technology

Design of harmonic filters to improve the operation of a PV system

By

Thomas Lionel MAKOSSO

Thesis submitted in partial fulfilment of the requirements for the degree of:

Master of Engineering in Energy (MEng Energy)

Department of Electrical, Electronic, and Computer Engineering

Faculty of Engineering and the Built Environment

Cape Peninsula University of Technology

Supervisor: Prof. Khaled Aboalez

Co supervisor: Dr. Ali Almaktoof

Bellville Campus

November 2021

DECLARATION

I, **Thomas Lionel MAKOSSO**, declare that the contents of the dissertation/thesis represent my own unaided work, and that the dissertation/thesis has not previously been submitted for academic examination toward any qualification. Furthermore, it represents my own opinions and not necessarily those of the Cape Peninsula University of Technology

Signed **Date**

Abstract

Renewable energy has been growing significantly, especially photovoltaic (PV) systems, PV system is a technology which can effectively help to overcome several issues. As the system is based on the conversion of the energy generated by the sun to electricity. The energy produced is clean, reliable and highly efficient. The main component of a PV system is the power electronics inverter, which is an electronic converter that converts DC current generated from the PV system to AC current fed to the local network at the point of connection. Because of the power electronic equipment present at the point of connection, there will be a generation of harmonic current which causes a power quality problem. Harmonics considerably affect the efficiency of the grid connected PV system. To achieve an acceptable distortion, increase the power quality and to reduce the harmonics, an LCL filter between the inverter and the grid has been designed. The mathematical concept is based on equations and the transfer function which describe the LCL filter. Transfer functions are the result of the ratios between various input to output Laplace-transformed complex currents and voltages. The most important transfer function for this LCL filter is from the inverter voltage to the grid current that is injected. It is important to note that the parameters mentioned above were designed under certain assumptions such as ideal power electronic switches, a constant DC link voltage and no perturbations in the output grid voltage. The passive damping is used to reach the stability in the voltage source inverter (VSI) based on LCL filter. By inserting passive elements into the filter structure, it changes the response and resonance frequency. So with parallel passive damping, the filter attenuation is decreased since this method adds a zero to the LCL filter transfer function. In the design and modelling approach, the filter is considered ideal, once magnetic and electrical losses are neglected. There are three major factors in the design which are: the grid side and inverter side inductance, as well as the capacitor. The capacitance value is a compromise between power factor decrease and injected current harmonic distortion. The expected value of the capacitance is by about 5% of the nominal power in order to avoid overrating the converter. In high power application like this study, the filter is not directly integrated into the converter. As the inductor current saturation is an important aspect. Then the calculation of the resonance frequency. It should be in a range larger than the grid frequency and smaller than the switching frequency, in order to avoid resonance in lower and higher harmonic orders.

In this thesis, a performance evaluation of the proposed system under different conditions, in terms of the THD in the output stage of the inverters, was undertaken. MATLAB/Simulink software package is used for the modelling and simulation.

Development of the simulation for the whole grid connected PV system using MATLAB/Simulink as a simulation tool to investigate the use of the designed filter to mitigate harmonics power of the system according to IEEE 519 standard. The results obtained reveal several information. It has been showed how the irradiance impacted the PV power output because from when the irradiance dropped the power does the same vice versa. The filter decreased the harmonic distortion rate from 25 to 2.39. The filter is very resilient, even besides the changes of step reference; it was able to maintain the harmonic percentage under a certain level.

Acknowledgements

I would like hereby express my sincere gratitude and appreciation to my Father and mother, my God, for giving me all that I needed to achieve this. I also wish to express my gratitude to the following:

- My family and friends, for their love, patience, prayers and understanding throughout this research study.
- My supervisor and co-supervisor , Prof. Khaled Aboalez and Dr. Ali Almaktoof for their motivation, support and guidance
- The academic and administrative staff of the Engineering Faculty of Cape Peninsula University of Technology for assisting in the completion of this survey.
- All my fellow colleagues for their encouragements.

Table of Contents

LIST OF FIGURES

LIST OF TABLES

Glossary of terms

Generator	An equipment that converts any form of energy into electrical one
IEEE 1547	Standard used regarding interconnected systems
Inverter	A device that offers a guaranteed security for any electronics equipments.
Megawatt (MW)	A unit of power (rate of energy consumption).
MATLAB	Used to develop models and analyse data
Model	A representation of real world system in a software environment such as Simulink for better understanding.
Simulink	A MATLAB based graphical environment for modelling and simulation
Filter	Are electronic circuits that remove unwanted frequency components from the applied signal, enhance unwanted ones, or both.
Harmonic	voltage and current frequency which are multiple of the main frequency of the supply system

LIST OF ABBREVIATIONS

AC	Alternating Current
VSI	Voltage Source Inverter
DES	Distributed Energy Source
FFT	Fast Fourier Transform
GCI	Grid Connected Inver
kW	Kilowatts
LCL	inductor capacitor inductor
MATLAB	Matrix Laboratory
MPPT	Maximum Power Point Tracking
MW	Megawatts
PCC	Point of Common Coupling
PV	Photovoltaic
VSI	Voltage Source Inverter
IEEE	Institute of Electrical and Electronics Engineers
P	Active Power
PLL	Phase Locked Loop
PI	Proportional Integral
PWM	Pulse Width Modulation
Q	Reactive Power
RES	Renewable Energy Sources
THD	Total Harmonic Distortion

LIST OF SYMBOLS

C_b	Base Capacitance
C_f	Filter Capacitor
f_g	Grid Frequency
f_{res}	Resonance Frequency
f_{sw}	Switching frequency
i_I	Inverter output current
i_g	Grid current
I_{ms}	Root mean square current
K_P	Proportional gain
K_i	Integral gain
L_i	Inverter side Inductor
L_g	Grid side Inductor
L_T	Total inductance
PF	Power factor
P_n	Nominal Power
R	Relation factor between inductances
R_f	Damping resistor
R_i	Inverter side inductor resistance
R_g	Grid side inductor resistances
V_i	Inverter output voltage
V_C	Filter capacitor voltage
V_{DC}	Nominal direct current voltage
V_g	Grid voltage
V_{ms}	Root mean square voltage
ω	Angular speed
ω_n	Natural frequency in rad/sec
Z_b	Base impedance

CHAPTER 1

INTRODUCTION

1.1 Introduction

1.2 Overview of the previous work

1.3 Statement of the problem

1.4 Objective of the research

1.5 Research design and methodology

1.6 Structure of the study

1.1 Introduction

Photovoltaic systems are on a growth trajectory that is expected to continue in the years to come. The grid efficiency, resilience and reliability are improved with the growing level of renewable energy penetration made possible by the development of smart grid technology (Y.Ibrahim, et al., 2017). PV system is one of the most important energy sources due to the fact that it is continuously available and cost-effective source of energy. The presence of smart grid will open up opportunities for solar power generation. Inverter is a major component in PV as it converts direct current to alternative current. There are three common types of PV inverter which are: rooftop solar PV, grid tied connected PV and battery back-up inverter (Badal & Das, 2019). Grid tied inverters are connected through power electronic voltage source inverters. The power electronic connection is generating harmonics (Chandra & Kulkarni, 2020) .To achieve an acceptable level of power quality, there is a need for a filter between the inverter and the network. A filter is used to minimize the harmonic currents , but some control difficulties may appear (Soonee, et al., 2019). And it leads to insecurity issues within the control framework and the resonance frequency between the inverter and the network. A few of the key impacts of voltage and currents harmonics on the diverse components of the grid are: decrease of framework proficiency, overabundance voltage and a current as a results of parallel and arrangement reverberation are crushed coming into shortening the life span of the components (Chishti, et al., 2020). Power electronics devices used converter of PV system cause harmonics problems. Solar irradiance, the inverter and temperature are the key elements of the PV performance and those elements affected the current profile and power generated (Xiao, et al., 2019). In this study, it is aimed to develop a modified model of filter which can improve the operation system of a PV system.

1.2 Overview of the previous work

In (Singh, et al., 2019), the authors designed a novel model of LCL filter for grid connected PV system. This LCL filter had an advantage to take off the peak near the resonance frequency. As a result, the proposed topology presented a design adaptability which assist optimization and reduction in terms of size in comparison to other configurations. In (Thomas & Mishra, 2019), the authors investigated the design procedures of a LCL filter for PV systems. Experimental results presented an appreciable compatibility with the research over the frequency range. From the IEEE recommended limits, the output harmonic current was sampled. The studied design procedure which allows the design of additional efficient and reliable filters in respect of the engineering standards.

In (Kanagatakshmi, et al., 2019), the authors introduced a straightforward, vigorous and efficient plan strategy of LCL filter parameter tuning. The proposed plan technique is to overcome the deficiencies of classical plan strategy, specifically, steady beneath diverse network setups and conditions. It took into thought the exactness of guidelines capacitors

values and proposes a basic plan strategy for the converter side of that maintains a strategic distance from the immersion issue.

In (Li & Li., 2020), the authors explored the plan rules for the inductor filter of a three phase grid PV inverters. With MATLAB/Simulink, a test was conducted with filters parameters. Both recreation and explanatory comes about illustrate the effectiveness and unwavering quality of the proposed technique were exploring. A subjective and quantitative dissect was made to choose the RMS value of fundamental and ripple component for the filter inductor current of grid-connected single-phase PV inverters. From the ripple of the current examination, design guidelines for filter inductor against the confinement were displayed. With an error beneath 4%, the proposed filter design guidelines were amazingly precise. In (Zhu, et al., 2019), the authors studied a coupled inductance calculation plan was presented for optimizing the control efficiency of a grid tied PV system. The forecast of the total harmonic distortion of the inverter grid side was made with the RMS ripple which inferred from the swell control misfortune. The proposed approach of arrangement was pertinent to the parameter plan for the LC and LCL coupled filter for negligible power loss.

In (Shi, et al., 2020), the authors examined investigation plan of LCL filter for association with the network. Diverse topologies of filters are examined along with their inconvenient. The frequency response curves were plotted in arrange to examine different detached damping strategies for LCL filter. And it came to the conclusion that the for medium and high power application LCL filter was favoured instead of LC or L filter as it offered more stability and productivity. In (Jiao, et al., 2019), the authors investigated new method to design the LCL filter for grid interfaced PV system. For getting the ideal filtering plan, fetched based minimization approaches on a taken cost per joules for each element are created. The viability of the proposed system was verified with the simulation results for a 10kVA grid connected inverter with LCL filter. The paper moreover tends to be conceivable effect of the outlines filter parameters. Firstly, it continued to a variation of inductance of the LCL filter and from that it identified the filter parameter which provided the lowest cost while meeting the harmonic standards requirements. Finally, the design method was validated with the experimental results. In (Loka & Parimi, 2020), the authors developed a novel kind of high filter named LCL-LC filter. The resonant frequency characteristic of the filter was examined, and a parameter plan strategy on the base of the characteristics was also displayed in the study. The parameter robustness of the proposed filter is analysed based on four-dimension design. Compared with the conventional LCL filter, this configuration of filter dissecting the filter performance beneath variations of several parameters without any cycle. From the tests, a 5kW grid connected converter prototype, it could make verification and a comparative analysis and discussion between LCL and LCL-LC filter. In conclusion, the experimental showed that the hypothetical analysis was precise and demonstrate that the LCL –LC filter was far more proficient than the

two others. In (Gong, et al., 2019), the authors investigated a new approach to LCL filter design for grid interconnected inverter systems. There was an expansion of a phase shifting transformer to the regular LCL filter, creating a PST-LCL filter with enhanced performance. The operation of the utility grid was significantly improved with the reduction of harmonics currents. The filter presented allows reducing the current total harmonic distortion to a desired range and gives the system the ability to respond to load and switching frequency changes quickly. In (Geetha & Subramani, 2018), the authors designed LCL filter for the mitigation of injected harmonics. The LCL filter was preferred as compared to the others because of its sizing and appreciable ripple component attenuation. The simulation results were conformed to the implemented hardware model. In the objective of solving the problem of filtering in three phase PV grid connected inverters, In (Keddar, et al., 2019), the authors established the design of L and LCL filter**.** The main component of the LCL filter(The inductance and the capacitance) was calculated by analysing the related constraints conditions. Two principals' ways of increasing the value of damping capacitor were looked into and an analyse was made over the impact on the stability and filtering property. The simulation results showed that the LCL filter was far more efficient than the L and LC filter. In the aim of increasing system stability, parallel resistor is more advantageous than series resistor.

1.3 Statement of the problem

Grid tied connected PV with power electronic interface raises some power quality issues. In ideal conditions, PV system should be able to operate without any problem relative to its power electronic interface. However, due to those power electronics components, harmonics are generated and significantly affect the power quality. The harmonics effect of distorting the supply voltage will affect the consumer appliances. In response to this problem, this study investigates the design of a filter for a more reliable and effective operation of PV systems. The aim of the study is to improve the design of the filter according to IEEE standard.

1.4 Objective of the research

The main research objective mainly to design and develop a LCL filter. Thereafter, an investigation on how to implement the proposed LCL filter is carried out to assess the impact on the performance of the PV grid tied system according to IEEE 519 standard.

To achieve the above objectives, the following steps are performed:

1. Literature study of the electronics components of PV system and the LCL filter.
2. Mathematical model of the LCL filter.
3. A performance evaluation of the proposed system under different conditions, in terms of the THD in the output stage of the inverters, was undertaken.
4. Development of the simulation for the whole grid connected PV system using

MATLAB/Simulink as a simulation tool to investigate the use of the designed filter to mitigate harmonics power of the system according to IEEE 519 standard.

1.5 Research design and methodology

1. Modelling of a PV system connected to the grid. It required a set of equations representing all the elements of the system that need to be studied.
2. The DQ theory of instantaneous power was used in the control strategy. The DQ theory had the advantage to be simple especially in analogical form as it only requires a simple filtering. The choice of the filter eventually included the choice of the capacitance and the inductance. All that in respect of the following criteria: Filter inductance values was chosen such that the combined size of the inductors is minimum, in the aim at providing an excellent quality current a sufficient attenuation was provided to the switching frequency component of grid current.
3. As software MATLAB /Simulink was used. With Simulink which is a simulation platform in multiple domains and the modelling of integrated systems. It provided a graphic environment and a library containing a set of blocks of modelling which allows an accurate design, implementation, and control.

1.6 Structure of the study

This thesis is comprised five chapters which are summarized as follows:

Chapter 2: presents the brief description of the PV system, power quality and the different filter topology. Four types of filters topology are presented . The various mode of operation in grid connected are developed, with a focus on the control of the entire configuration system. Power quality issues are also introduced based on IEEE standards.

Chapter 3: presents the mathematical description of the system. From the Design of the LCL filter and the required calculations to the implementation of the control strategy of the MOSFET inverter. The mathematical model of the LCL filter and the major elements to consider during its design are presented. And the DQ theory used in the model is explained as well as the perturb and observe algorithm used for the maximum power point tracking from the output of the PV system.

Chapter 4: presents the modelling and analysis of LCL filter. The LCL filter modelling steps are carried out starting from: design factors (Output current ripple, current harmonics) and the criteria, then the calculation process of the filter, Which is based on finding three main elements which are: the capacitance, the grid and inverter side inductance. After that the output of the inverter as well as its control strategy are defined and calculated. In order to control the current and voltage while running the entire system.

Chapter 5: is where the simulations of the proposed model are implemented in MATLAB/Simulink based the parameters calculated in chapter four. Voltage and current output from the inverter before and after insertion of the LCL filter are runned under two distinct scenarios. The first scenario with a constant power of 210kW and the second one with a step reference change of 300kW. As well as the dq command of the controller are runned and all those results are clearly analysed and discussed.

Chapter 6: is the discussion and final conclusion of the study and an overview of the future work.

CHAPTER 2

Literature Review

2.1 Introduction

Through the years, conventional energy sources have proven their effective potential to stimulate the economic progress. But, the primary energy sources have increased in 2012 due to the fast depletion of conventional energy sources and the growing demand (Han, et al., 2019). Because of the primary energy sources affect considerably the environment; many related organizations have strongly promoted research in order to develop cleaner plants (Chen, et al., 2019). As a matter of fact, renewable energy prices, social and are gradually decreasing and the monetary and coverage mechanisms had to help the sizeable dissemination of sustainable markets for renewable energy systems are swiftly evolving (Pan, et al., 2020). It is evident that the future of energy will be orientated to renewable energy. So, moving to renewable energy will be profitable by decreasing gas emission, and make sure of the reliable, timely, and cost-efficient delivery of energy. Energy security can be secured with renewable energy (Wang & Jin, 2018).

Renewable energy is generally theoretically inexhaustible source of energy like wind, sun and water (hydropower). The development of well-established technologies like hydro, as well as growing technologies like wind and sun has been spread rapidly. It has raised interest and opened up opportunities (Li, et al., 2020), figure 2.1 shows on overview of some sources.

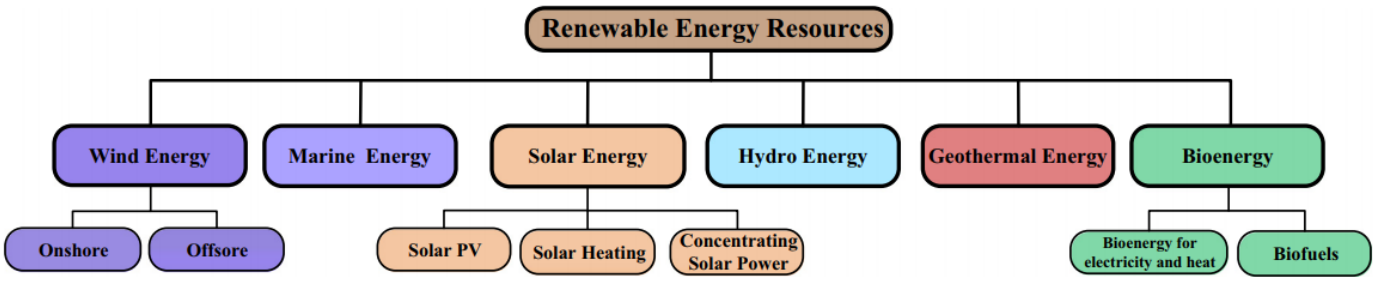

Figure 2.1: Overview of renewable energy sources (Zeb.K, et al., 2018)

2.2 Grid connected PV systems

A conventional solar panel allow photons and particles of light, to knock electrons free from atoms and from that generate a certain flow of energy. That's saying that the photovoltaic cells have the ability to convert the energy in sunlight to electricity, especially direct current. Studies revealed that the total amount of energy arriving on the earth surface in the form of sunlight is approximately 10000 times the world's energy requirements (Dhaneria, 2020)

2.2.1 Mode of operation in grid connected

Grid connected inverters have different applications, they can be utilized as interfacing for technologies to associate to the utility grid as displayed in Figure 2.2.High efficiency and low cost are the greatest advantage of grid connected inverters (Xiang, et al., 2018). More often, the grid connected inverters are classified into two principal categories which are: single and the two stages or multistage. But, the more stages you have the lower the effectiveness of the GCI is. A two stage is composed of a DC/DC to DC/AC stage (Kan, et al., 2020). The two stages have for fundamental objective to elevate the PV voltage, track the most extreme power. The direct to alternative current stage is critical. As compared to the two stages, the one stage as it were comprised the DC to AC (YI, et al., 2019). The single stage incorporates a straightforward topology and has a simple topology and high efficiency besides the fact that it has the control strategy tougher to execute. In difference, the two stage needs a bearing algorithm program that is much less demanding, since several commands are executed by two steps that are distinct (Tomar, et al., 2018).

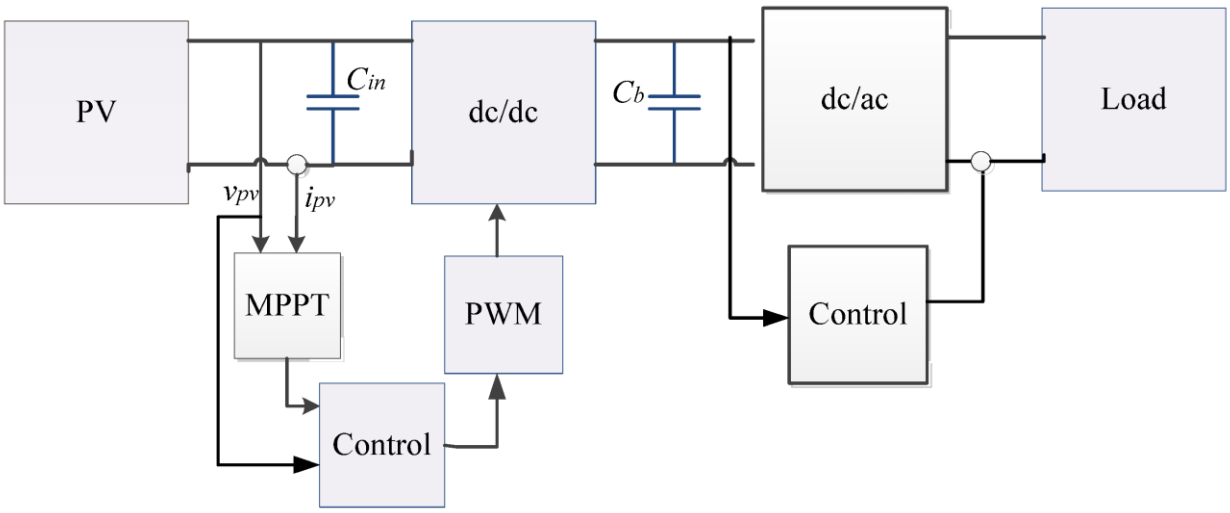

Figure 2.2: Grid connected system (Zhao.N, et al., 2018)

2.2.2 Components of grid connected PV system

It is made of a 210kW PV system, boost converter, three phase MOSFET inverter, LCL filter and the grid.

2.2.3 Conditioning units

Solar power conditioning units (PCU) are integrated systems composed of a solar charge controller, an inverter and a grid charger. They are purposed to control the power generated from the source and proceed to a change from DC to a high AC quality power and then injects it in the grid (Tarek, et al., 2019). With power systems there are two power processing stages

which are the single and two stage. The control tasks are performed by the inverter. .In addition, the control given with the two stages system is more adaptable, but needs extra cost and cut in the accurateness of the system (Singh & Tiwari, 2020).

2.2.4 Control of the injected current

PCUs have for objective to ensure that the current which goes to the grid has a similar frequency and provide phase shift at a point of common connection with the permissible limits. Besides, the harmonic contents must be within the limits indicated in the standards.

2.2.5 Islanding detection and protection

It is characterized as the fact of an isolated part of the system from the grid remains powered. In common, the benchmarks need that PCUs of the PV systems should terminate the infusion of power into the grid under unusual operating conditions.

2.3 Different types of inverter

AC loads are distinguished into single and three phases, regarding of how the system is fed. This might be by a single phase or three phases (Jian, et al., 2019) Distinctive sorts of inverter setups are used to drop the power fluctuations. Those disturbances linked to the voltage that happen both in single and three-phase system share almost the same highlights (Ayalew, et al., 2020). In addition, movement toward PQ is possible with voltage unbalance compensation. The mitigation of the reactive power is the principal concern of the single-phase system (Fajri, et al., 2018), (Zhang, et al., 2018). Grid connected inverter topology in a single-phase system, as a rule does not have expansive capacities mostly used in little scale in renewable energy (Narendra, et al., 2019) The single phase GCI has more capacities has more advantage as express prior and are mostly used in residential PV system (Singh & Panigrahi, 2020). More ever the strategies of identifying harmonic in three bases GCI is known to be more often than just an unbalanced source (Narendra, et al., 2019). Subsequently, three phase GCI have many point of interest which makes it satisfactory for a large set of development. Three phase system in high power applications, presents several advantages:

1. It decreases the stress of the inverter switches.
2. Diminishes in estimate and evaluations of reactive components.
3. The frequency of the output current increases.
4. It makes an unchanging dispersion of losses.

2.4 Topology of grid connected inverter configurations

Primarily inverters are controlling electronic interface systems which are utilized in changing over DC to AC power (RajaMohamed, et al., 2019). The inverter interfaces to the network guaranteeing its execution to the most efficient power.

2.4.1 Centralized topology

It is the most developed of all. It is used in expensive PV framework with up to a few megawatts. In this topology, a single inverter is associated to the PV system as seen in Figure 2.3. The most beneficial with this technology is its amazing low cost. But, it has low reliability as the failure of the inverter will halt the PV system from operating. In addition, there is a basic control incident inside the case of mismatch between the modules and halfway shading. It overhauls the quality of a central topology.

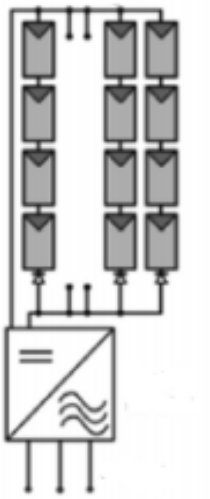

Figure 2.3: Centralized topology (Zeb.K, et al., 2018)

2.4.2 String topology

Each string is related to an inverter which upgrades positively the quality. In addition, the misfortunes because of the halfway shading are decreased because each string can work at its claim greatest power point. Figure 2.4 shows the String topology configuration. It boosts the adaptability within the plan of the PV system. As a rule, the power rating needs to be up to 222-3kW.The most drawback is the expanded fetched due to the growth in the number of inverters.

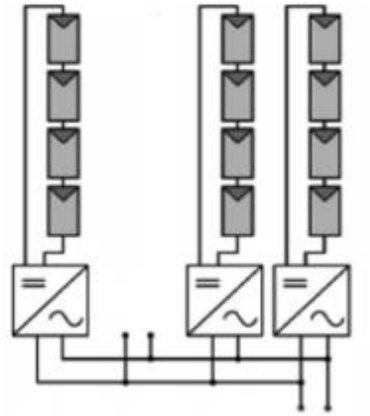

Figure 2.4: String topology (Zhao.N, et al., 2018)

2.4.3 Multi string topology

Each string is related to a DC-DC converter for taking the maximum control point and voltage intensification. The converters are at that point associated to a single inverter by means of a DC transport as seen in Figure 2.5. This topology combines the preferences of string and centralized topologies and uses a central inverter for decreasing the cost. In any case, the quality of the system is less efficient as compared to the other configurations.

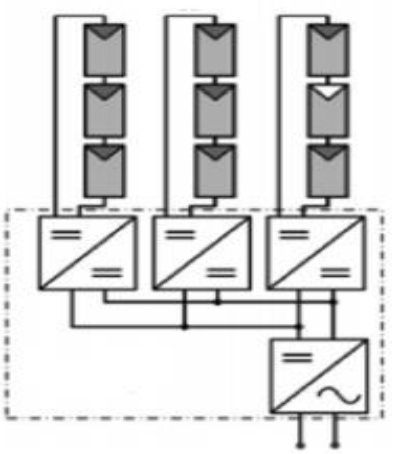

Figure 2.5: Multi string topology (Zhao.N, et al., 2018)

2.4.4 Modular topology

Usually the foremost topology. They additionally referred to as ‘AC’ modules since an inverter is inserted (See Figure 2.6). It has numerous point of interest such as lessening of losses because of the fractional shading, superior checking for module disappointment, and adaptability of array design. In any case, it is appropriate for low power applications (up to 500W) and its cost is moderately high. Additionally, the lifetime of the inverter is decreased

since it is introduced within the open discuss with the PV module, hence expanding its thermal stressInvalid source specified..

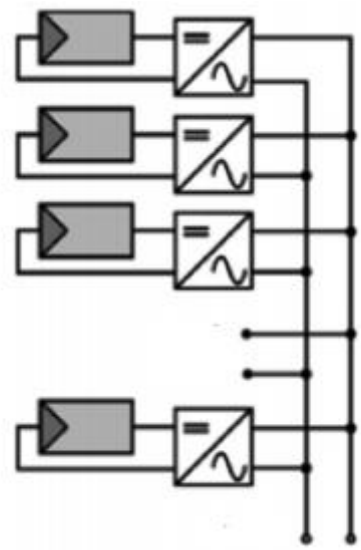

Figure 2.6: Modular topology

2.5. Power quality

It is defined as a steady supply voltage that remains under the prescribed or adequate range of power (Wang & Ren, 2018). In addition, the principal goals of the quality control were to improve the services towards the consumer and then limited the complaints. In (Surendran, et al., 2017), the author outlined two principals' factors which important in the quality of electricity which are: the continuity of supply and the quality of the voltage. In (Mehiri, et al., 2017), the author notes down the causes and the impact of the voltage distortion and discussed the nature, parameters and consequences of rapid voltage sags, asymmetry and variations and harmonics and transient overvoltage (Jain & Signh, 2019). Nowadays, there is not a general agreement about the meaning of "power quality. Table 2.1 shows some IEEE standards.

Table 2.1: Different IEEE Standards

IEEE Standards	Description
IEEE P1366	Guide for electric distribution reliability indices
IEEE 1100	Recommended for powering and grounding sensitive electronic equipment
IEEE 1159	Practice for monitoring electric power quality
IEEE 519	Harmonic mitigation

In table 2.2, the IEC standards have been introduced as the study is executed according to those standards as well.

Table 2.2: IEC Standard (Y.Ibrahim, et al., 2017)

Issue/Parameter	IEC 61727	IEC 1547	IEEE 929
Nominal Power	10kW or smaller PV systems connected to the utility grid	This standards covers distributed resources as large as 10MVA	10kW or less
Harmonic currents(Order h) limits	(3-9)4.0% (11-15)2% (17-21)1.5% (23-33)0.6%	<4% for (2-10)th <2% for (11-16)th <1.5% for (17-22)th <0.6% for (23-34)th	(3-9)4.0% (11-15)2% (17-21)1.5% (23-33)0.6%
Voltage range for normal operation	85-110% (196-253V)	_	88 – 110% of nominal voltage. Inverter should abnormal response.
Frequency range	$50 \pm 1Hz$	_	59.3-60.5Hz

The electromagnetic compatibility characterizes the capacity of equipment to operate without presenting unfortunate electromagnetic disturbances to anything in that environment. In spite of all the benefits presented by the PV system to the utilities, it does not exclude the fact that there are a few potential issues related with grid-connected systems**.** Line or high frequency converters can do conversion from DC to AC. A great sinusoidal waveform can be created with such converters (Mazaheri, et al., 2019). The system is put into work at a specific power factor with a control on the converter. A voltage drop occurs while transmitting reactive power; it comes within the utility network that is more likely to generate a low voltage at the output of the feeders (Errouissi & AL Durra, 2019).The inverter can distinguish a fault or power outage within the utility grid and disconnect from the system. If a fault occurs the converter proceeds to function (Singh, et al., 2019)When generating a high DC voltage by interfacing a gigantic amount of PV cells in series. With the usage of a DC/DC converter, there is a possibility to prevent that issue (Venkatasamy, et al., 2018).

Back in the years, the harmonic problem has been incomparable with the excessive use of converters, in this manner having a coordinate impact on the power quality (Ayalew, et al., 2020). As a matter of fact, harmonics issues are recognized as a sort of unsettling influence which are not directly linked to the network linear, decides a steady modification of the voltage and current sinusoidal waveform, like components that are subject to changes such as the frequency (Moftah, et al., 2016). Decrease within the quality of power and the performances

of other equipment affected by harmonics will be modified because of PV generator associated. (Sorte, et al., 2021). With the harmonic voltage distortion, the operation of the static converters may be affected. Harmonic filters are then necessary (Mazaheri, et al., 2019). The utility grid can be subject of losses and potential breakdown of equipment. (Errouissi & Al Durra, 2019). Those effects are continuous; they ought to not be disregarded. Later inverter hardware working on PWM switching is exceptionally great, producing slight harmonics.

2.5.1 Harmonic filtering

Those past 20 years, semiconductor has known an incredible progress which has promoted some control applications which incorporate high voltage DC system (Kishor, et al., 2021)In any case, the operation mode of these devices is making issues , they keep on expanding in spite of the fact that these systems improved and made up modern applications (Neira, et al., 2020). This equipment which draws non-linear current f on the front conclusion. There is interference between the line voltages of the distribution system because of the impedance (Jain & Singh, 2020).The neutral line, which is not designed to transport a huge amount of power, can encounter voltage unbalance and excessive currents due to the presence of power electronic devices (Jadhav & Patil, 2020). Business clients that draw over the top reactive power are usually punished by energy provider.

The level of harmonic is limited by upgrading the output waveform of the inverter along these lines, decreasing the size of the filter Invalid source specified.**.** Mainly, passive and active filters mitigate harmonics distortions in most of the systems. Various research is progressing to improve the power distribution system and grid requirements as the efficiency and quality of voltage is concerned. The utilization of LCL filter in GCIs has increased more consideration because of its upgraded ability to decrease harmonics coming from the utilization of a switching frequency that is as negligible as possible lower. Moreover, the electromagnetic interference is limited by the IEEE-1547 and 519 standards. Generally, used for the GCI but the output from this inverter is an adjustable voltage, in this way, it is fundamental to mitigate the harmonics prior connection to the grid as respect of the network prerequisite. The LCL filter is generally used because of its upgraded ability to mitigate harmonics, power consumption is insignificant and electromagnetic impedance is limited. Different researches are yet progressing on the examination of the LCL design.

2.5.2 Filter Topology

It aims to supply the grid with current of proper quality. The choice of the inverter to be used depends also on the weight and the efficiency of the filter. LCL filter has the ability to dampen high frequency noise. Reason why, the author considered a filter design in (Sorte, et al., 2021).

Firstly, the filter ought to have an uppermost inductive behaviour to allow the appropriate running of the VSI whenever it is connected to the utility grid (Dhaneria, 2020) In addition, the on grid PV system creates PWM carrier and side-band voltage harmonics. This voltage may conduct to the progression from the current into the grid. It will influence other sensitive loads (Neira, et al., 2020) So as to fit in with those prerequisite, a filter containing a basic inductor is the straightforward way out. When it comes to huge applications, the switching frequency is low (Jain & Singh, 2020).

In the aim of meeting the demand of the grid, then reducing the harmonic, additional high value input are needed (Kakkattukunnumal, et al., 2019). Moreover, the energetic reaction of the system can be worse. But even more reduced inductance can match the criteria, but there is still should be adhere to as recommended by the standards (Hinsui & Sangtuntong, 2019). English band potential drop harmonics is a favoured approach. The accurate final outcome can be obtained making use of as tiny as possible of inductors. For power converter switching at hundred Hz, this solution is absolutely applicable as it generates PWM harmonics that have a very low frequency (Chandra & Kulkarni, 2020).

The major problem comes with the insecurities created by some of the few particular harmonics. Subsequently an imply of decreasing or dispensing these harmonics (Tiwari & Singh, 2020).

2.5.3 LC Filter

The output and the grid voltage are synchronized together and the PWM inverter provides ripple current to the grid (Panday, 2020). The output current of the inverter generates a high switching frequency which is undesirable; in order to remove it there is a connection of the output filter introduced. The choice of the suitable inductor for the filter depends on the current ripple. The ripple current mostly represents 10% to 15% of rated current. The Figure 2.7 below shows a LC filter (second order) with an attenuation of -40dB/decade.

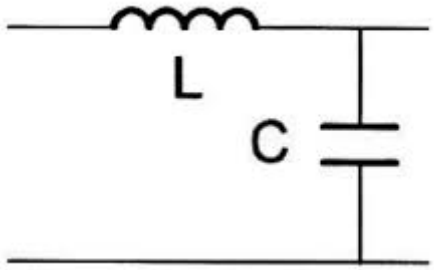

Figure 2.7: LC Filtre (Jiao, et al., 2019)

The design of the capacitor depends on the reactive power supplied by the capacitor at fundamental frequency.

The elimination of the switching frequency is carried by a shunt element, especially since the decrease of the attenuation is of the inverter switching components is realized by the L filter the choice of the shunt component is crucial as it allows the generation of low reactance at the switching frequency (Abujubbeh & Marazanye, 2019). But, the only requirement is that the component presents large magnitude impedance. The proposed shunt element is a capacitor.

2.5.4LCL filter (third order)

Among the well-known advantages for high power applications is the presentation of the LCL filter presented in Figure 2.8. It yields better decrease of inverter switching harmonics compared to other filter configurations. An increasing perplexing current control procedure allowed the stability to be maintained regarding of the system. Due to grid voltage harmonics there is a generation of interference which leads of resonance risks. It is quite difficult to meet the IEEE 519 standards requirements with a low inductance on the inverter side (Mohapatra, et al., 2020). The LCL filter offers the possibility of realizing a minimized harmonic distortion levels with lower switching frequencies and less total energy stored (Battacharya & Kumar, 2019) .

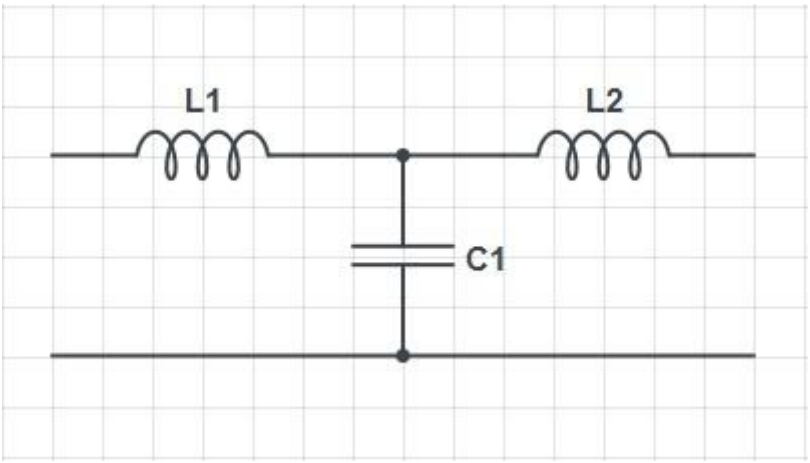

Figure 2.8: LCL filter (Wang.B, et al., 2017)

2.6 Summary

This chapter discussed the PV system in general, power quality and the filter topology. The t grid connected PV system represents a core part of this system. A general description, operation mode and different types of topology are presented in order to provide an overview of different scenarios. And the final part of this chapter was particularly focused on the power quality. The harmonic impact on the grid was highlighted as well as the common types of filter used to mitigate its effects. In the following chapter , the mathematical description of the entire configuration is studied.

CHAPTER 3

Mathematical description of the three phase grid tied PV system

3.1 Description of the system.

In the Figure 3.1, the three-phase grid connected PV system is presented. The PV system of 210kW is the main source of power, and then it is made of a boost converter with raises the voltage to 600V.After that the three phase MOSFET inverter converts that DC power to AC. The LCL filter is present between the grid and the inverter in order to decrease the total harmonic distortion that is more like to occur.

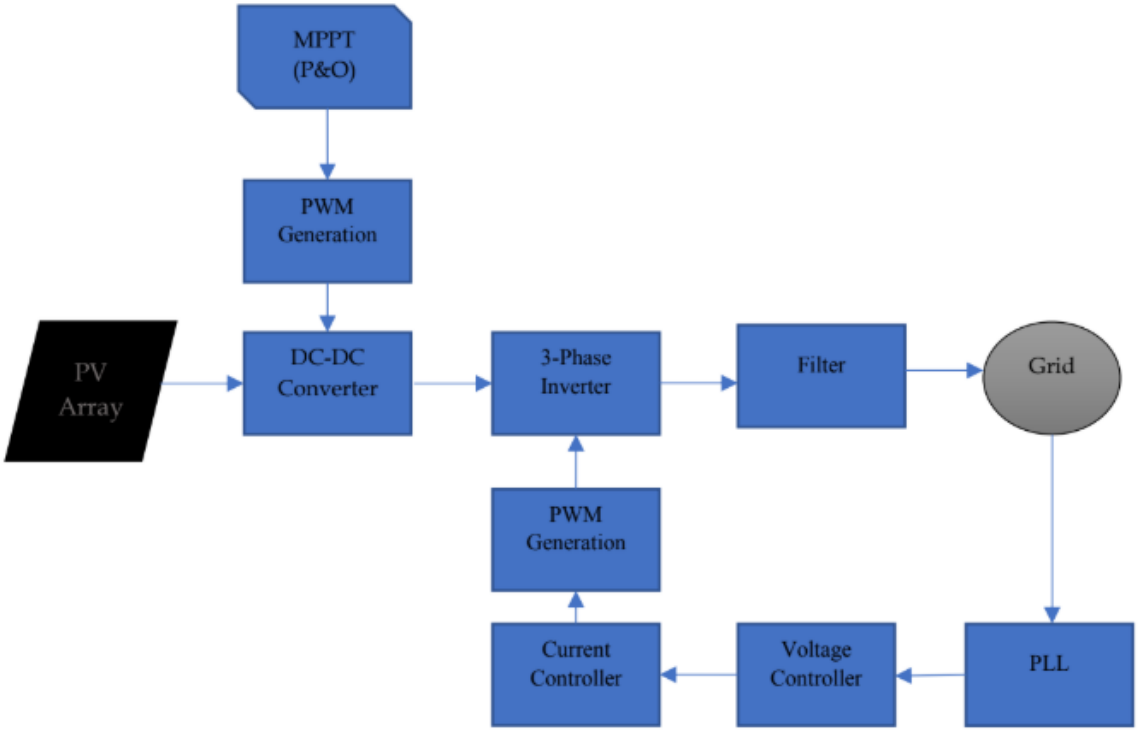

Figure 3.1: Block diagram of the three-phase grid connected PV system.

3.2 Mathematical description of the Photovoltaic system

A solar module is a panel made of photovoltaic cells. The modelling of the solar cell gives more accurate details on the power output (Mao.L, 2018). A photovoltaic array comprises many solar cells wired in series or in parallel. An equivalent model of photovoltaic module is shown in Figure 3.2.

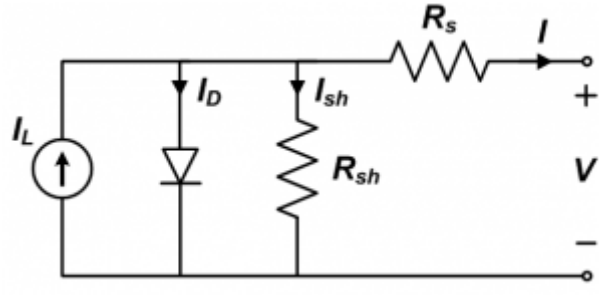

Figure 3.2 equivalent circuit of a photovoltaic module (Zeb, et al., 2019)

The Kirchhoff law is applied to calculate the current generated from the PV

$$I = I_L - I_D \quad (3.1)$$

The diode current is given by the Shockley equation:

$$I_D = I_O \left[exp^{q\left(\frac{V - IR_S}{\gamma K T_C}\right)} - 1 \right] \quad (3.2)$$

Where I_D and I_L are the diode and photoelectric current related to a given condition of radiation and of temperature;

V refers to the output voltage $[V]$,

I_O Represents an index of the cell failing;

γ Series resistance of the cell;

q Electric charge;

K Boltzmann's constant;

T_C is the module temperature;

If (2) is substituted into (1) the following equations are obtained, that represents the I-V module characteristics.

$$I = I_L - I_O \left[exp^{q\left(\frac{V - IR_S}{\gamma K T_C}\right)} - 1 \right] \quad (3.3)$$

In (3.4) a model with predefined values γ, R_S, I_O and I_L is proposed. The model completed below with the following equations considers all PV conditions:

$$I_O = I_{Oref} \left(\frac{T_c}{T_{Cref}}\right)^3 exp\left[\left(\frac{qE_g}{k\gamma}\right)\left(\frac{1}{T_{Cref}} - \frac{1}{T_C}\right)\right] \quad (3.4)$$

$$I_L = \left(\frac{G}{G_{ref}}\right)\left[I_{Lref} + \mu_{ISC(T_C - T_{Cref})}\right] \quad (3.5)$$

Where E_g represents the energy gap;

G is the radiation$[W/m^2]$;

G_{ref}The radiation under standard conditions$[W/m^2]$;

I_{Lref} Is the photoelectric current$[A]$;

T_{Cref} The module temperature $[K]$;

μ_{ISC}The temperature coefficient of the short circuit current$[A/K]$.

The current source generates the photo current I_L which is directly proportional to the solar irradiance$F_s[W/m^2]$; T_a ambient temperature and the two output parameters: current $I_S[A]$ and voltage$V_s[V]$. The p-n transition area of the solar cell can be assimilated to a diode (Yadzani.A, 2014). From the Kirchhoff's current law, the characteristics equation of the one diode model. Equation represents the (I_L) photocurrent equation:

$$I_L = P_1 \times G\left[1 + P_2 \times (G - G_{ref}) + P_3 \times \left(T_j - T_c\right)\right] \quad (3.6)$$

Where $G_{ref} = 1000\ W/m^2$;T_{cref}= 298.15K; $P_1[Am^2/W]$, $P_2[m^2/W]$, $P_3[1/K]$

The current I_D is calculated with:

$$\begin{cases} I_D = I_O\left[exp^{\left(\frac{q}{af \times Ns \times k}\right)\left(\frac{V - IR_S}{\gamma KTc}\right)} - 1\right] \\ I_{Sat} = P_4 \times T_j^3 \times exp^{\left(\frac{-E_g}{k.Tj}\right)} \end{cases} \quad (3.7)$$

Where the ideally factor a_f is 1. $N_S\ is$ the number of cells in series; R_s represents the series resistance, the band gap is $E_g[eV]$, $P_4[A/K^3]$ represents the correction factor. $P_4[A/K^3]$.

The following equation expresses the diode reverse saturation current Io:

$$I_O = \frac{V + IR_S}{R_{Sh}} \quad (3.8)$$

3.2.1 The first empirical model for PV cells

The experimental model was actually developed in order to facilitate the determination of One and two-Diode-Model parameters. Then, the experimental model was introduced. It is based on a small number of parameters V_{OC}, I_{SC} and maximum power P_{MPP} of the solar panel.

$$\left(\frac{\partial V_{oc}}{\partial T_j}; \frac{\partial V_{oc}}{\partial E_s}; \frac{\partial I_{sc}}{\partial T_j}\right) \quad (3.9)$$

The equation that describes the I-V characteristic is given by:

$$I = I_L - I_D \quad (3.10)$$

With the use of the approximation $I_{ph} \approx I_{SC}$ and substituting the constant $q/a_f.k.T_J$ with A, equation (3.10) becomes:

$$I = I_O\left[1 - exp[(V + I_S R_S)]\right] \quad (3.11)$$

If I_s= 0 and V= V_{OC} and the factor A can be calculated by:

$$I=0= V_{oc}= \frac{1}{A}\ln\left(\frac{I_{sc}}{Io1}\right) \rightarrow A = \frac{1}{V_{oc}} \ln\left(\frac{I_{sc}}{Io1}\right) \quad B = \ln\left(\frac{I_{sc}}{Io1}\right) \quad (3.12)$$

In standard test conditions (T_C = 25°C and G_{ref}= 1000W/m^2) the ratio I_{SC}/ I_{Sat}can be approximated with 10^9

Replacing A and making the notation B = $\ln\left(\frac{I_{sc}}{Io1}\right)$ the value of the expression of V_S becomes:

$$V = V_{oc} \times \left[1 + \frac{1}{B} ln(I_0 - I)\right] - R_S I \quad (3.13)$$

At maximum power point (MPP) the value of the current I_s is $I_{MPP}$and S = P_{MPP}/I_{MPP}. The values of R_S and I_{MPP}can be obtained by resolving the system:

$$V = P_{MPP}/I_{MPP} \quad (3.14)$$

$$\begin{cases} \frac{P_{MPP}}{I_{MPP}} = V_{oc} \times \left[\frac{1}{B} + ln(I_{SC} - I_{MPP})\right] - R_S I_{MPP} \\ \frac{P_{MPP}}{I_{MPP}^2} = \frac{V_{OC}}{B} \times \left(\frac{1}{I_{SC} - I_{MPP}}\right) + R_S \end{cases} \quad (3.15)$$

3.2.2 The second empirical model for PV cells

From the current equation, the second model is as follow**:**

$$I(V) = I_{SC}\left(1 - \left(\frac{V}{Voc}\right)^k\right) \quad (3.16)$$

Where

$$k = \ln\left(1 - \frac{I_1}{I_{Sc}}\right) / ln\left(\frac{V_1}{V_{oc}}\right) \quad (3.17)$$

And the values (I_1,V_1) are found at the MPP. This method is efficient because of the accuracy of foreseeing the MPP using the equations:

$$\begin{cases} V_{MPP} = V_{OC} \times \frac{1}{(1+k)^{1/k}} \\ I_{MPP} = I_{SC} \times \frac{k}{1+k} \end{cases} \quad (3.18)$$

With an increase of 25°C in temperature. These relations can be modelled such as:

$$\begin{cases} V(G, T_c) = V_o + \frac{nkt}{q} ln\left(\frac{G}{G_{ref}}\right) - n\alpha\left(T_c - T_{cref}\right) \\ V(G, T_C) = I_o\left(\frac{G}{G_{ref}} - \beta\left(T_c - T_{cref}\right)\right) \end{cases} \quad (3.19)$$

3.2.3 Power conditioning units

It can be described as an integrated system that is made of a charge controller, an inverter and a grid charger. The power conditioning system regularly monitors the state of Battery Voltage, Solar Power output and the loads (R, et al., 2019). It has to check the requirements of the subsystem are conforming.

3.3 Boost converter

It is found to be a core component on renewable energy system (wind and solar). The efficiency of such system is crucial to counterbalance the effect of the efficiency. This power electronic equipment boosts the low voltage level to high level from. And it also contributes to improve both the power extracted from the PV and voltage at the output. Figure 3.3 shows an average boost converter having an input and output voltage.

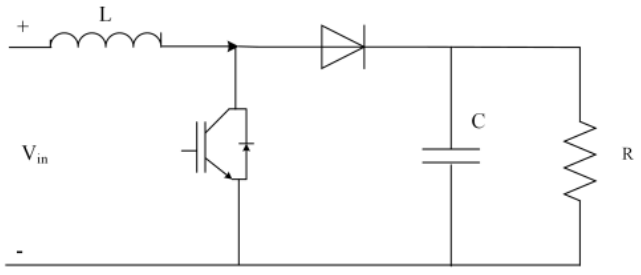

Figure 3.3: Average boost converter (Wijesinghe, 2019)

The output voltage during the on-span would be over the capacitor. The estimation of the capacitor ought to be adequately enormous enough to keep up the steady voltage over the

heap. During off switching the inductor will release the opposite way, which will make a diode become forward one-sided. The relation between the output and the input voltage is:

$$V_o = \frac{V_{in}}{(1-D)} \tag{3.20}$$

Here D = T_{on}/T_{switch} represents the duty ratio of the on-time interval over the switching time T, V_{in} and V_0 are the input and output voltage. It can be set in either continuous conduction mode (CCM) or discontinuous conduction mode (DCM). In CCM, the inductor current will be a non-zero value, though in DCM, the inductor current accomplishes zero worth.

While designing the converter; the capacitor and inductor are the most significant components. With the following equation an appropriate design can be carried out:

$$\text{L} = \frac{D(1-D)V_{DC}}{f_{sw}\Delta IL} \tag{3.21}$$

Here D is the duty cycle, V_{DC} is the DC-link voltage, f_{sw} is the switching frequency. L is chosen thinking about the most extreme estimation of ΔIL conceivable. The inductor choice is performed dependent on (2.7). The D value ends up being 0.125 for the information voltage of 700 V from 2.7. Thus, an inductor value of 5 mH is selected for the boost converter. The choice of the capacitor is extremely crucial in respect of the overall performance of the boost converter. It ought to be adequately enormous to diminish the oscillation towards the grid. The equation 2.8 details how to the select the capacitor value for the boost converter.

$$C_{dc} = \frac{P_{in}}{wV_{DC}\Delta_{DC}} \tag{3.22}$$

Controllers are used to track the voltage. The instability of the current may occur issues for the converter.

Figure 3.4 presents the schematic of the external PV voltage regulator and the internal current regulator. The reference voltage for the external voltage loop is set by the MPPT output. This guarantees that the voltage will be kept up at the most extreme output voltage. The error from the external loop produces the current signal, which

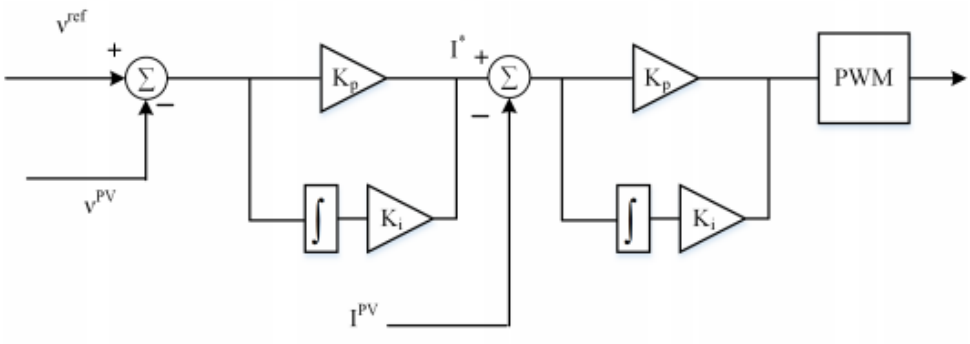

Figure 3.4: PV regulator (Elmelegi, et al., 2019)

Turns into the reference for the inward control loop.

3.4 Voltage source inverter

The representation of a three phase two level VSI is presented in Figure 3.5. It is mostly used for active filtration purposes, motor drives and uninterrupted power supplies for the control of the voltage with the pulse width modulation.

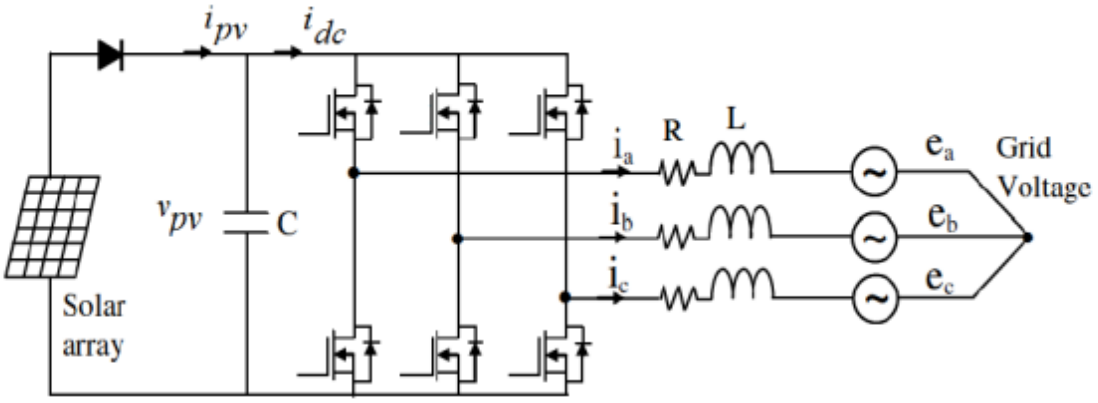

Figure 3.5: Voltage source inverter (VSI) (Noman, et al., 2019)

The Switching states operation of the three-phase inverter is presented in Table 3.1. There are six modes of operation for each cycle with duration of 60^0. If the MOSFET Q1 is switched on, the terminal a is connected to the positive input of the DC source. And MOSFET Q4 goes on terminal a brought to the negative terminal of the DC source.

Table 3.1: Switching states for three phase voltage inverter

State No.	S1	S2	S3	S4	S5	S6	V_{ab}	V_{ca}	V_{bc}
1	1	1	0	0	0	1	V_S	0	$-V_S$
2	1	1	1	0	0	0	0	V_S	$-V_S$
3	0	1	1	1	0	0	V_S	V_S	0
4	0	0	1	1	1	0	V_S	0	V_S
5	0	0	0	1	1	1	0	$-V_S$	V_S
6	1	0	0	0	1	1	V_S	$-V_S$	0
7	1	0	1	0	1	0	0	0	0
8	0	1	0	1	0	1	0	0	0

The following equations represent the three-phase grid voltages having peak voltage V and angular frequencyω. The conditions can be expressed as follows:

$$v_a = V\cos(\omega t) \tag{3.23}$$

$$v_b = V\cos\left(\omega t - \frac{2\pi}{3}\right) \tag{3.24}$$

$$v_c = V\cos\left(\omega t + \frac{2\pi}{3}\right) \tag{3.25}$$

The representation of the equation in space form

$$\begin{pmatrix} \frac{dI_a}{dt} \\ \frac{dI_b}{dt} \\ \frac{dI_c}{dt} \end{pmatrix} = \begin{pmatrix} \frac{-R}{L} & 0 & 0 \\ 0 & \frac{-R}{L} & 0 \\ 0 & 0 & \frac{-R}{L} \end{pmatrix} \begin{pmatrix} I_a \\ I_b \\ I_C \end{pmatrix} + \left(\frac{1}{L}\right) \begin{pmatrix} u_a - v_a \\ u_b - v_b \\ u_c - v_c \end{pmatrix} \tag{3.26}$$

Equation (2.10) after transformation :

$$\begin{pmatrix} \frac{dI_d}{dt} \\ \frac{dI_q}{dt} \end{pmatrix} = \begin{pmatrix} -R & WL \\ -wL & R \end{pmatrix} \begin{pmatrix} I_d \\ I_q \end{pmatrix} - \frac{1}{L}\begin{pmatrix} v_d \\ v_q \end{pmatrix} + \frac{1}{L}\begin{pmatrix} u_d \\ u_q \end{pmatrix} \tag{3.27}$$

As presented in (2.11), I_d, I_q, u_d , u_q, V_d and V_q are d-axis and q-axis components respectively of the current, output and the grid voltages respectively,

$$u_d = \mathrm{L}\frac{dI_d}{dt} + Ri_d - wLi_q + v_q \tag{3.28}$$

$$u_q = \mathrm{L}\frac{dI_q}{dt} + Ri_q - wLi_d + v_d \tag{3.29}$$

Once the PI controller is introduced, (3.28) and (3.29) become

$$u_d = \left(K_p + \frac{K_i}{s}\right)(i_d^* - i_d) - wLi_q + v_d \quad (3.30)$$

$$u_q = \left(K_p + \frac{K_i}{s}\right)(i_q^* - i_q) - wLi_d + v_q \quad (3.31)$$

3.5 Mathematical description of the LCL filter

The mathematical equations and transfer function describe this LCL filter and contribute to find the grid and inverter side inductance as well as the capacitor values.

3.5.1 LCL Model and Justification

Transfer functions are the result of the ratios between various input to output Laplace-transformed complex currents and voltages. The transfer function is given by:

$$H_{LCL}(s) = \frac{I_{g(s)}}{V_{i(s)}} = \frac{CR_Ds+1}{D_{LCL}} \quad (3.36)$$

Where

$$D_{LCL} = CL_1L_2s^3 + (CL_1R_2 + CL_2R_2 + CL_1R_D + CL_2R_D)s^2 + (L_1 + L_2 + CL_1L_2 + CR_1R_D + CR_2R_D)s + (R_1 + R_2) \quad (3.37)$$

Obtained using this equation

$$H_{LCL}(s) = C\,(sI\ sI - A)^{-1}B + D \quad (3.38)$$

Where A, B, C and D are matrices

Neglecting all the three resistances the equation is reduced to

$$H_{LCL} = \frac{1}{CL_1L_2s^3 + (L_1 + L_2)s} \quad (3.39)$$

3.5.2 Mathematical Model of LCL Filter

The mathematical model of the proposed LCL filter is based on (F, et al., 2020), (H, et al., 2021), (U, et al., 2020), (P, et al., 2020) previous work. Figure 3.6 describes the topology of an LCL filter; V_i and V_g are the inverter and grid voltage, respectively. Similarly,I_i,I_c and I_g are the inverter, capacitor and the grid currents, respectively.

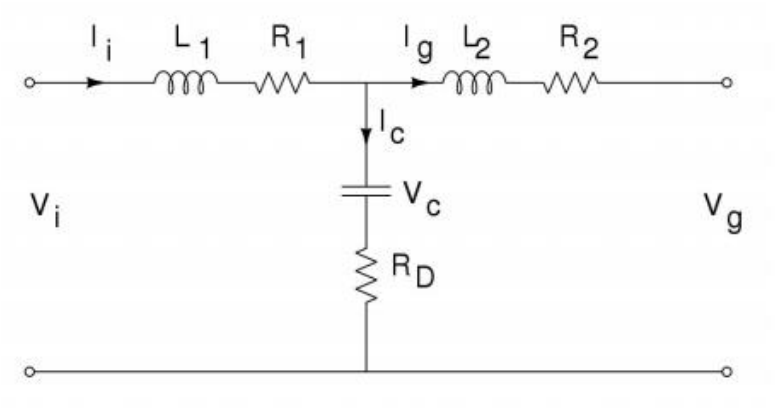

Figure 3.6: Single Phase LCL Filter Schematic

With the Kirchhoff's voltage and current laws from Figure 3.6, the following is obtained

$$I_i - I_g = I_c \tag{3.40}$$

$$I_c = C \times \frac{dV_c}{dt} \tag{3.41}$$

$$V_{L1} = L_1 \times \frac{dI_i}{dt} = V_i - R_1 I_i - V_C - R_D I_C \tag{3.42}$$

$$V_{L2} = L_2 \times \frac{dI_g}{dt} = V_c - R_2 I_g - V_g - R_D I_C \tag{3.43}$$

Rearranging these get to:

$$\frac{dI_i}{dt} = \frac{1}{L_1}\left[-(R_1 + R_D)I_i + R_D I_g - V_C + V_i\right] \tag{3.44}$$

$$\frac{dI_g}{dt} = \frac{1}{L_2}\left[-(R_2 + R_D)I_i + R_D I_i + V_C - V_g\right] \tag{3.45}$$

$$\frac{dI_g}{dt} = \frac{1}{C}\left(I_i - I_g\right) \tag{3.46}$$

The representation of the equation in space form

$$\begin{pmatrix} \frac{dI_i}{dt} \\ \frac{dI_g}{dt} \\ \frac{dV_c}{dt} \end{pmatrix} = \begin{pmatrix} \frac{-(R_1+R_D)}{L_1} & \frac{R_D}{L_1} & \frac{-1}{L_1} \\ \frac{R_D}{L_2} & \frac{-(R_2+R_D)}{L_2} & \frac{1}{L_2} \\ \frac{1}{C} & \frac{-1}{C} & 0 \end{pmatrix} \begin{pmatrix} I_i \\ I_g \\ V_C \end{pmatrix} + \begin{pmatrix} \frac{1}{L_1} & 0 \\ 0 & \frac{-1}{L_2} \\ 0 & 0 \end{pmatrix} \begin{pmatrix} V_i \\ V_g \end{pmatrix} \tag{3.47}$$

It defines the state vector as:

$$x = \begin{pmatrix} I_i \\ I_g \\ V_C \end{pmatrix} \tag{3.48}$$

And the input vector as

$$u = \begin{pmatrix} V_i \\ V_g \end{pmatrix} \tag{3.49}$$

The output (Y) equation:

$$y = I_g = (0)I_i + (1)I_g + (0)V_C + (0)V_i + (0)V_g \quad (3.50)$$

The state space representation of this equation is

$$y = \begin{pmatrix}0 & 1 & 0\end{pmatrix}\begin{pmatrix}I_i \\ I_g \\ V_C\end{pmatrix} + \begin{pmatrix}0 & 0\end{pmatrix}\begin{pmatrix}V_i \\ V_g\end{pmatrix} \quad (3.51)$$

Then the complete space state form of the LCL filter model as:

$$\begin{aligned}\dot{x} &= Ax + B \\ y &= Cx + Du\end{aligned} \quad (3.52)$$

Where the matrices A, B, C and D defined as

$$A = \begin{pmatrix}\frac{-(R_1+R_D)}{L_1} & \frac{R_D}{L_1} & \frac{-1}{L_1} \\ \frac{R_D}{L_2} & \frac{-(R_2+R_D)}{L_2} & \frac{1}{L_2} \\ \frac{1}{C} & \frac{-1}{C} & 0\end{pmatrix} \quad (3.53)$$

$$B = \begin{pmatrix}\frac{1}{L_1} & 0 \\ 0 & \frac{-1}{L_2} \\ 0 & 0\end{pmatrix} ; C = \begin{pmatrix}0 & 1 & 0\end{pmatrix} ; D = \begin{pmatrix}0 & 0\end{pmatrix} \quad (3.54)$$

Need for a third order filter. Here in, a comparison is made between a first order filter (L) and a third order filter (LCL) one and show that a third order filter is superior at attenuating higher harmonic frequencies.

Defining:

$$X_L = w_g L \quad (3.55)$$

$$X_1 = w_g L_1 \quad (3.56)$$

$$X_2 = w_g L_2 \quad (3.57)$$

$$X_C = \frac{1}{w_g C} \quad (3.58)$$

$$w = hw_g \quad (3.59)$$

And using the equation 3.39 the harmonic transfer function is obtained as

$$H_{LCL}(jhw_g) = \frac{I_{g(jhw_g)}}{V_i(jhw_g)} \quad (3.60)$$

$$= \frac{-j}{hw_g\left(L_1+L_2-L_1L_2C \quad h^2w_g^2\right)}$$

Therefore

$$\left|H_{LCL}(jhw_g)\right| = \left|\frac{I_{g(jhw_g)}}{V_i(jhw_g)}\right| \quad (3.61)$$

$$= \left|\frac{-j}{hw_g\left(L_1+L_2-L_1L_{2C}h^2w_g^2\right)}\right| \quad (3.62)$$

$$= \left|\frac{1}{hw_g\left(L_1+L_2-L_1L_{2C}h^2w_g^2\right)}\right| \quad (3.63)$$

$$= \left|\frac{1}{h\left[X_1+X_2-\frac{h^2X_1X_2}{X_C}\right]}\right| \quad (3.64)$$

When C = 0 it reduces into a L filter with L = $L_1 + L_2$ and the above transfer function is

$$\left|H_{LCL}(jhw_g)\right| = \frac{1}{hXCL} \quad (3.65)$$

Considering $X_{1,}X_{2,}$ and $X_{c,}$ in per unit values as:

x_1= x_1= 0.05 ; x_1= 135.115

Ensuring that the resonant peak is far away from both the power frequency (60 Hz) and the switching frequency (15000Hz) ($10f_g < f_{res} < 0.5f_{sw}$).

It is important to note that the parameters mentioned above were designed under certain assumptions such as ideal power electronic switches, a constant DC link voltage and no perturbations in the output grid voltage. Additionally, the formula for estimating THD is approximate.

3.6 Summary

In this chapter, the mathematical description and all the related equations of each and any components of the three phase MOSFET inverter such as the PV , Boost converter , an overview of mathematical modelling of LCL filter have been explained. In order to have a clear overview of the elements that was used during the design of the system. In the following chapter, more specific and deep mathematical modelling and design of the LCL filter are investigated.

Chapter 4:

Modelling and Analysis of the LCL Filter

4.1 Introduction

4.2 LCL Filter design

- 4.2.1 LCL design factors
- 4.2.2 System parameters
- 4.2.3 LCL filter design criteria
- 4.2.4 LCL Filter design process

4.3 Three phase MOSFET inverter

- 4.3.1 Output Filter
- 4.3.2 Three phase grid connected inverter synchronization
- 4.3.3 Grid synchronization using PLL technique
- 4.3.4 Design of synchronous reference PLL

4.4 Control of the PV grid tied system

- 4.4.1 Maximum power point tracking
- 4.4.2 DQ theory
- 4.4.3 PWM modulation

4.5. Three phase connected VSI

- 5.1 Model of current controller
- 5.2 Design of PI based control scheme

4.6 Conclusion

4.1 Introduction

This chapter focuses mainly on the methodology used to design the LCL filter (Wang.M, 2016). The calculation process of the LCL filter is based on the capacitance and the grid and inverter side inductance. All that taking into account the following parameters: voltage line to line, DC link voltage, resonance frequency and grid voltage which plays a key role in order to design an efficient filter. Then a control strategy based on PI controller is implemented to provide high quality power.

4.2 LCL Filter design

It involves several which are: the parameters, mathematical modeling, design factors and criteria.

4.2.1 LCL design factors

A simple first order L filter is not only bulky but fails to meet the requirements for harmonic attenuation. Output current ripple, current harmonics sourced by MOSFET inverter, series fundamental drop, desirable power factor, resonance frequency, control stability are among the factors that need to be taken into consideration.

4.2.2 System parameters

The following system parameters mentioned in Table 4.1 are considered for designing the requisite LCL filter:

Table 4.1: Nominal system parameters

f_g	Grid frequency
f_{sw}	PWM carrier frequency
w_{res}	Resonance frequency
P_n	Rated active power
E_n	Line to line RMS voltage
V_{DC}	DC link voltage
L_1	Inverter side inductor
L_2	Grid side inductor
C	Capacitor
R_d	Damping resistance
V_g	Grid voltage

4.2.3 LCL filter design criteria

The following criteria are extremely important while designing a LCL filter:

a. High attenuation
b. Improved performance
c. Cost effectiveness

4.2.4 LCL Filter design process

In most three phase inverters, the three phases are identical and separate from each other. And leads to three decoupled systems, each of which is like a single phase inverter. In the inverter design with an LCL filter, each phase will have three main components, two inductances and a capacitance, as well as series resistances. Each of these inductors is wound on isolated cores. In Table 4.2, the values presented are used in the rest of the calculation.

Table 4.2: Parameters used in Filter calculation

Parameters	Nomenclature	Values
Voltage line to line	V_{LL}	380V
Voltage at DC link	V_{DC}	600V
Resonance frequency	f_w	30000Hz
Nominal Power	P_n	210000kW
Inductance	Li	Henry

$$Z_b = \frac{V_{LL}^2}{P_n} \quad (4.1)$$

$$= \frac{380^2}{210} = 687.61\Omega$$

$$Z_b = \frac{1}{Z_b \times \omega_n} \quad (4.2)$$

$$= \frac{1}{2\pi \times 50 \times 687.61}$$

C_b= 462 μF

The inverter side inductor mainly minimizes the ripple current of the MOSFET inverter.

$$X_{LPU} = \frac{L\omega_n}{Z_b} \quad (4.3)$$

$$= \frac{Z_b \times X_{LPU}}{\omega_n} \quad (4.4)$$

$$= \frac{0.05 \times 686}{2\pi \times 50} = 10.91 \text{ mH}$$

$$\Delta I_{Lmax} = \frac{V_{DC}}{8 f_\omega L_i} \quad (4.5)$$

$$= \frac{600}{8 \times 30 \times 109.1}$$

$$\Delta I_{Lmax} = 2.29\ A$$

$$L_g = r L_i \quad (4.6)$$

$$L_{Total} = \frac{X_{L\_Total} \times Z_b}{\omega_n}$$

$$= \frac{686.6 \times 0.09}{2\pi 50} = 19.67\text{mH}$$

So $L_g = L_{Total} - L_i$ (4.7)

$$L_g = 19.67 - 10.91 = 8.67 \text{ mH}$$

$$C_f = \beta . C_b \quad (4.8)$$

$$= 0.05 \times 462 = 23.1 \mu F$$

The filter resonance frequency can be calculated as follow

$$f_{res} = \frac{1}{2\pi} \sqrt{\frac{L_i + L_g}{L_i \times L_g \times C_f}} \quad (4.9)$$

$$= \frac{1}{2\pi} \sqrt{\frac{19.97}{8.67.10^{-3} \times 10.91.10^{-3} \times 23.1 \times 10^{-6}}}$$

$$f_{res} = 2055 \text{ Hz}$$

$$\omega_{res} = 2\pi \times 2055 = 12911.9\ rad/sec$$

The requirement of about 5% is perfectly matched. The damping resistor value is calculated as follow:

$$R_f = \frac{1}{3 \times 2\pi \times 2055 \times 23.1 \times 10^{-6}}$$

$R_f \quad = 1.12\,\Omega$

The Table 4.3 presents the LCL filter parameters found after calculation.

Table 4.3: LCL filter parameters

Parameter		Value
Grid side inductor	L_g	8.67 mH
Inverter side inductor	L_i	10.91
Filter capacitance	C_f	$23.1\mu F$
Damping resistor	R_f	1.12Ω
Resonance frequency	ω_{res}	$12911.9\,rad/sec$

4.3 Three phase MOSFET inverter

The model developed is a bidirectional inverter. At the necessary yield voltage and recurrence, the three phase inverter effectively flips over DC power into AC. It is noticeable utilizing diverse inverter configurations and control plans with each having their advantages and downsides.

Fundamentally for this plan, a six switch three-stage inverter topology is utilized. The configuration is comprised of three equal branches, and comprise of two switches in arrangement on each branch with cells comprised of a semiconductor and a diode associated in against equal. The age of the three stage AC yield happens in the middle of the two switches of each branch. The design is straightforward, broadly utilized, with an awesome geography to incorporate extra inverter highlights then draw more attraction. The contribution of the inverter is in type of an ideal, adjusted, three-stage voltage source, associated with the matrix. This depiction of the inverter model depends on an essential thought that the utility voltage is hardened. The working state of the exchanging capacity to ensure that the channel inductor current isn't upset, have to be adhered by the switches

The Exchanging of the inverter is constrained by PWM in an appropriate arrangement to create an unfiltered yield voltage. Sinusoidal heartbeat width balance (SPWM) is utilized to create the exchanging signals for the inverter at the ideal greatness and recurrence by contrasting a three-stage sinusoidal wave. The recurrence of the MOSFET is due to the recurrence of the three-sided signal coming about into beats which drives the entryway signal. Equations represent the voltage wave form.

$Va_{ref} = A\sin(2\pi ft + \theta)$ (4.10)

$Vb_{ref} = A\sin\left(2\pi ft + \theta - 120^{\circ}\right)$ (4.11)

$Vc_{ref} = A\sin(2\pi ft + \theta + 120^{\circ})$ (4.12)

Where A represents the amplitude, f frequency, θ phase shift. In Table 4.4, the switching pattern of the pulse width modulation is described from the first to the sixth switch

Table 4.4: PWM switching pattern.

Switch	Applicable Sine wave	$V_S > V_T$	$V_S < V_T$
S_1	V_a	ON	OFF
S_2		OFF	ON
S_3	V_b	ON	OFF
S_4		OFF	ON
S_5	V_c	ON	OFF
S_6		OFF	ON

There can be a short output over the DC source, which could harm the switches or the total inverter when there is concurrent exchanging. In any case, exchanging is performed dynamically; the mix of the two corner to corner switches gives the unfiltered yield voltage. when the yield voltage is 0 . A comparing numerical inverter was introduced to depicting the power electronic VSI design to build up the control framework. The regulators 'factors are the energy stockpiling components.

4.3.2 Output filter

A three-phase MOSFET inverter connected by a DC source which is the PV system are depicted in Figure 4.1.

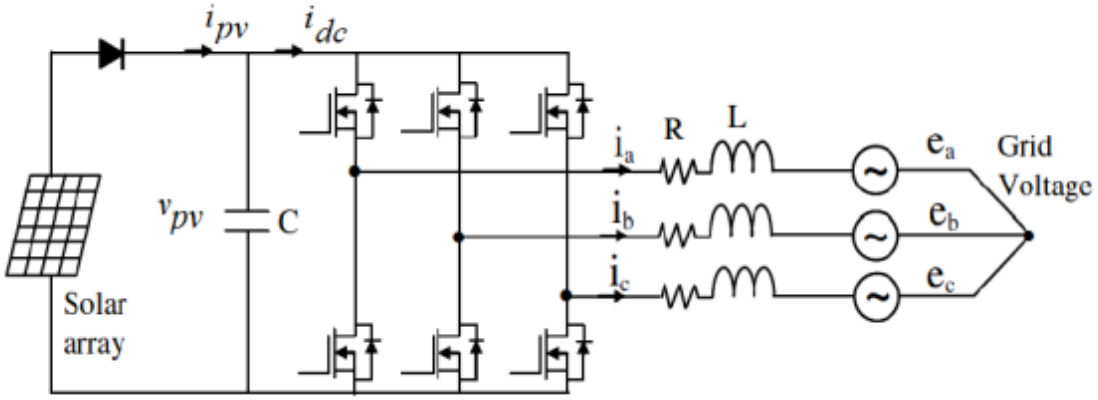

Figure 4.1: Three phase MOSFET Inverter

The following equations express the current from each phases as well as the voltage

$$i_a = -\frac{R}{L}i_a - \frac{1}{L}e_a + \frac{v_{pv}}{3L}(2S_a - S_b - S_c) \quad (4.13)$$

$$i_b = -\frac{R}{L}i_b - \frac{1}{L}e_b + \frac{v_{pv}}{3L}(S_a + 2S_b - S_c) \quad (4.14)$$

$$i_c = -\frac{R}{L}i_c - \frac{1}{L}e_c + \frac{v_{pv}}{3L}(S_a - S_b + 2S_c) \quad (4.15)$$

$$i_{dc} = i_a S_a + i_b S_b + i_c S_c \quad (4.16)$$

$$\rightarrow v_{dc} = \frac{1}{C}i_{dc} - \frac{1}{C}(i_a S_a + i_b S_b + i_c S_c) \quad (4.17)$$

4.3.3 Three phase grid connected inverter synchronization

The Park transformation is used for two main reasons. First, the dimensions of the mathematical model of the inverter are too extensive. And last, facilitate the control process of the entire system**.** The synchronous reference frame deals perfectly with non-ideal conditions of the grid.

4.3.4 Grid synchronization using PLL (phase lock loop) Technique

It can be assimilated to a tool, which permits one sign to follow the other. The current control circle depends on the PI (corresponding indispensable) regulator and the PLL is liable for providing the signs to it. The stage point, recurrence and voltage of the network is distinguished by the PLL. This arrangement of PLL is comprised of the stage discovery and the circle channel. Execution of the stage recognition can be accomplished by utilizing *abc* to *dq* change in the three-stage framework. On the other hand, the elements of the framework are controlled by the circle channel. In any case, the transfer speed of the channel is an understanding between the presentations of the channel what's more, the time reaction. Subsequently, nature of the lock and the PLL elements is exceptionally affected by the boundaries of the loop filter. The Figure 4.2 shows the PLL control loop configuration.

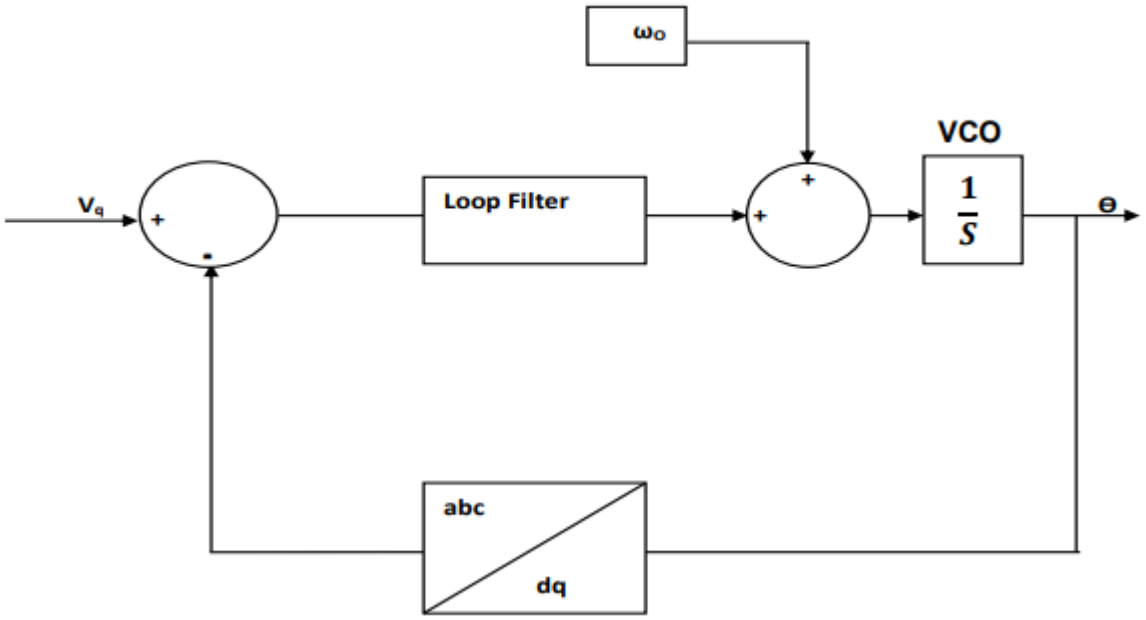

Figure 4.2: PLL control loop (Battacharya & Kumar, 2019)

4.3.5 Design of synchronous reference PLL

The PLL framework is impacted by the mutilations present in the utility organization when it is used for framework associated applications. A plan for quick elements will then again deliver a yield which can synchronize quickly to the information. Consequently, when the synchronization framework is being planned. In the event that the technique is utilized for control purposes, at that point a moderate unique strategy can be executed. And, if the synchronization strategy is utilized in network checking, for example, recognizing framework deficiencies, a quick powerful framework ought to be utilized. A tuning method for the dq-PLL regulator is given in this manner. The settling time and damping proportion of the framework can be gotten to through this strategy. In this manner, in view of these boundaries, a low elements or quick elements framework can be planned. The tuning strategy is gotten from the exchange capacity of linearized *dq*-PLL portrayed

The transfer function of the closed loop dq PLL system is represented as follow:

$$H_C(s) = \frac{\theta_O(s)}{\theta_i(s)} \quad (4.18)$$

$$H_C(s) = \frac{K_f(s)}{s+K_f(s)} \quad (4.19)$$

$$H_e(s) = \frac{\sigma(s)}{\theta_i(s)} \quad (4.20)$$

$$H_e(s) = \frac{s}{s+K_f(s)} \quad (4.21)$$

$$K_f(s) = K_p\left(\frac{1+s\tau}{s\tau}\right) \quad (4.22)$$

$$H_C(s) = \frac{2\zeta\omega_n s + \omega_n^2}{s^2 + 2\zeta\omega_n s + \omega_n^2} \quad (4.23)$$

Where

$$\omega_n = \frac{s^2}{s^2 + 2\zeta\omega_n s + \omega_n^2} \quad (4.24)$$

Where $\omega_n = \sqrt{\frac{K_p}{\zeta}}$

$$\zeta = \frac{K_p}{2\omega_n} \quad (4.25)$$

4.4 Control of the PV grid tied system

In order to properly run the PV grid tied system, the control of both the maximum power output from the PV and current and voltage in the voltage source inverter.

4.4.1 Maximum power point tracking

The Heuristic search with the Perturbation and observation technique reveals to be more straight and simple than the other techniques.

Maximum power point tracking is a technique which basically compares the voltage and the power. And make the system reacts accordingly.

The improvements of calculation of the P&O consist of fluctuating the voltage reference of the converter input current. In the long run, the measure of the intensity changed over from the panel is estimated. On the off chance that is more huge than the force estimated beforehand, the voltage reference is gradually expanded in a similar extent, and if not it is decremented (Matiyali, et al., 2019). In the goal of discovering the proper MPPT issue are utilized to improve energy change. The Figure 4.3 shows the case of P and O algorithm.

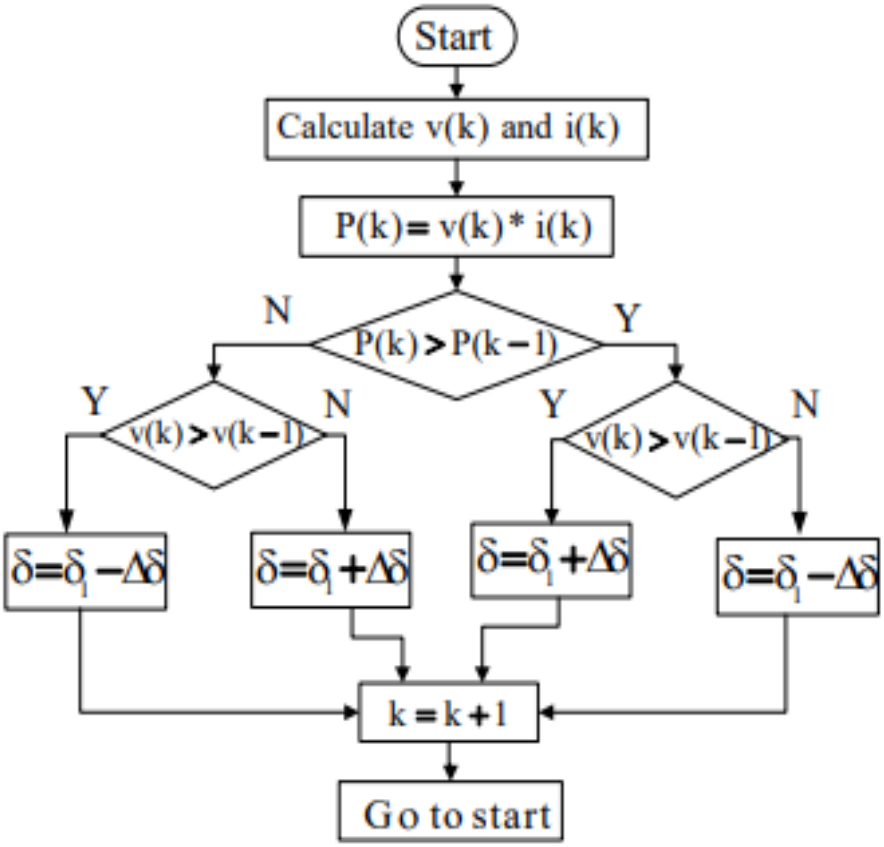

Figure 4.3: P&O algorithme (Remache, et al., 2019)

4.4.2 DQ theory

The DQ theory depends on the time space reference signal strategies. It allows performing the operation in steady state for generic voltage and current waveforms. Additionally, the simplicity of calculations gives this theory more efficient, which involves only algebraic calculation (Burlaka, et al., 2019).

The Park transform is a 2-2 transform that also has a reference angle input. If the reference angle θ is rotating at the same speed as a frequency component of the two-dimensional input to the Park transform, the output of the latter corresponding to this frequency component will be time invariant. Regarding to Park transformation relation between three phase source current (a-b-c) and the d-q reference co-ordinate current

$$\begin{pmatrix} I_{ld} \\ I_{lq} \\ I_{lo} \end{pmatrix} = \sqrt{\frac{2}{3}} \begin{pmatrix} \cos\theta & \cos\left(\theta + \frac{2\pi}{3}\right) & \cos\left(\theta - \frac{2\pi}{3}\right) \\ -\sin\theta & -\sin\left(\theta + \frac{2\pi}{3}\right) & -\sin\left(\theta - \frac{2\pi}{3}\right) \\ \frac{1}{\sqrt{2}} & \frac{1}{\sqrt{2}} & \frac{1}{\sqrt{2}} \end{pmatrix} \tag{3.32}$$

Where θ represents the angular position of the synchronous reference. The currents in the synchronous reference can be split into two terms as:

$$\begin{cases} i_{ld} = \widetilde{i_{ld}} \\ i_{lq} = \widetilde{i_{lq}} \end{cases} \tag{3.33}$$

The power filter reference currents will be then:

$$\begin{bmatrix} i_{fd}^{*} \\ i_{fq}^{*} \end{bmatrix} = \begin{bmatrix} i_{ld}^{*} \\ i_{lq} \end{bmatrix} \tag{3.34}$$

In the objective of finding the passive power filter current in three phase system, this relation can be used as follow:

$$\begin{pmatrix} I_{fa} \\ I_{fb} \\ I_{fc} \end{pmatrix} = \sqrt{\frac{2}{3}} \begin{pmatrix} \cos\theta & -\sin\theta \\ \cos\left(\theta + \frac{2\pi}{3}\right) & -\sin\left(\theta - \frac{2\pi}{3}\right) \\ \cos\left(\theta + \frac{2\pi}{3}\right) & \sin\left(\theta + \frac{2\pi}{3}\right) \end{pmatrix} \begin{bmatrix} i_{fd}^{*} \\ i_{fq}^{*} \end{bmatrix} \tag{3.35}$$

4.4.3 PWM modulation

The modulation allows getting an output that varies with minimum losses. In (Kapil.N & Rushiraj.G, 2016), the authors show that a meticulous choice of the PWM strategy can highly enhance the inverter output harmonic spectrum by moving harmonic components to higher frequencies.

4.4.3.1 Different PWM techniques modulation

Several techniques based on pulse width modulation (PWM) strategies are frequently used today's electrical engineering world as part of the control of solid-state power supplies. The inconvenient of PWM are that voltage and current ripple levels depends on the duty cycle, switching frequency and properties of the load (Venkatranaman & John, 2020). There is a possibility for the PWM output to be smoothed and averaged to limit these effects by using an appropriate high switching frequency and by using an additional passive filter. PWM power control systems realization can be made easier with semiconductor switches. In either the on or off state, there is only little power dissipated by the switch (Sun.K, et al., 2018).

4.4.3.2 Inverter side control

The use of power electronic converters has significantly improved the ability to extract maximum power from PV panels, and to condition the power supplied to the load so as to achieve high power quality, and to meeting the requirements for grid-tied operation. There are several power electronic converter schemes used for controlling the PV system output power (Zhao.N, et al., 2018). The electrical generator type determines the power electronic scheme

to apply, the load supplied by the PV system, and the control topologies used in the system. The inverter unit represents the most important unit in the PV systems for the AC power interfacing purposes. This study will focus on three -phase inverter development particularly in the inverter gate-drive and the controller side. So, it is important looking at the components and the functioning of the inverter before starting the development process (Wang.B, et al., 2017).

4.4.3.3 Modulation strategy

The stability and repeatability of inverter performance characteristics are essential both for reliable PV system performance and in order to determine the parameters in the performance model. The quality of the inverter output voltage depends on the number (nth) of harmonics and the magnitude of each harmonic that exists in the output voltage (Lopez.I, et al., 2016). The inverter output quality can be measured by several parameters; the most important ones are the magnitude of individual (nth) harmonics (HFn), and the total harmonic distortion (THD). The PWM technique is the principal technique used in this study. Its principle of operation is to turn the switch between supply and load on and off at a fast pace (to perform PWM), the frequency of which is referred to as the carrier frequency. PWM is mostly associated to the duty cycle (δ), which represents the percentage ratio of the switch on time (ton) to the full period time (Tsw).

4.4.3.4 Method for inverter current control

Control of current is an important issue in power electronic circuits, especially in DC-to-AC inverters where the objective is to generate a sinusoidal AC output whose magnitude and frequency can both be controlled. The main function of the current controller is to improve the voltage stability and to ensure the non-circulation of current amongst the converters (Monge.S, et al., 2017). In addition, the output voltage should have acceptable transient performance without poor dynamic response, undesirable overshoot or undershoot. In the other side, total harmonic distortion needs be as low as possible and below the standard threshold values.

4.4.3.5 Grid side control

The research encourages the idea of incorporating a small-scale renewable energy power supply into domestic dwellings as part of the power network. In this perspective, a large number of small-scale decentralized power supplies would be connected to the power network, which may possibly increase the complexity of the power supply control systems (Zeb.K, et al., 2018). If an existing grid is connected only to a large centralized power plant, the voltage at the common coupling point cannot be significantly modified by a small-scale decentralized power supply. In (Rashidi.F & Farahani.H, 2017), the author specified that the inverter must not oppose or attempt to regulate the voltage at the point of common coupling

(at which point the grid voltage is measured). Inverter's power quality will then be defined by its output current quality. Indeed, most power networks are three-phase systems. Therefore, distributed resources are connected to the grid via an isolating three-phase transformer to eliminate zero-sequence components in three-phase systems.

The inverter side controller uses grid parameters which can be measured at the inverter-grid common coupling point without extensive communications. With the droop function method, it turns out to have an efficient usage of small-scale renewable energy sources. In this method, controlling the inverter output power by controlling the voltage magnitude and phase shift depends on locally-measured instantaneous information. In this method, the grid parameters are used as reference at the common coupling points for all distributed generators.

4.4.3.6 Carrier frequency selection

For both component sizing reduction of the filter and also minimize the effect of harmonics, the PWM switching frequency should be as high as possible. But, during the transitions between on and off states of power semiconductor switch devices, both device current and device voltages are non-zero, and considerable power is then dissipated in the switches (Zarepour.E, et al., 2015). An improved switching device should provide a faster slope during turn-on and turn-off to avoid a switching overlap (shoot-through) case. For ideal switching elements, rise and fall times should be symmetrical and be small, a trade-off between switching losses and electromagnetic interference. Voltage swings at the bridge output from one voltage amplitude extreme to the other are mainly resulted from PWM. Within any PWM smoothing filter, the amplitude of the switching ripple in the output voltage will decrease by a specific percentage. In the modern engineering world, power switching devices designed for low to medium-power inverters can operate at relatively high frequencies in the tens of kHz range.

4.4.3.7 Decentralized power supply

Most power plants are built in a large scale due to a number of economic, safeties, logistical, environmental, geographical and geological factors. There are many disadvantages with such centralised systems, including:

- The high level of dependence on non-renewable fuels.
- Impact on the environment.
- Transmission and distribution losses.
- Higher cost of the generation plant, transformers, transmission, and distribution network.

In the last two decades, standards of living have considerably risen. This is explained by the considerable changes occurred in the energy usage patterns of buildings, due in part to

widespread utilisation of refrigeration and electric heating in domestic appliances (I.molino, 2014). It follows that, distributed generation stations are another approach within the power network to provide further electrical power to the utility. Distributed generation reveals to be a possible solution to meet the increased demand for power. The construction of power lines is decreased in size as well as number (Kumar.J, et al., 2019).

4.5 The three-phase connected VSI method

By and large, two existing procedures can be used, which are voltage strategy and current control technique. The DC precariousness is certainly not a significant issue when planning the GCI as this can be overwhelmed by executing a quick current regulator. The Air conditioner current via the structure of control is limited. Likewise, the stage point and the plentifulness of the line current for the VSI control the genuine and responsive force with regard to the PCC voltage. Thus, the VSI isn't under the danger of over-burden circumstances because of current control framework. The regulator, additionally has some different advantages such as strength against jumble in boundaries of the VSI and AC framework, an exceptional dynamic of execution and sophisticated control accuracy.

4.5.1 Model of current controller

As recently referenced, the usage of the coordinated reference outline is favoured in view of its points of interest. The dq-outline change is utilized all together to show the three-stage framework associated PV framework in the coordinated edge. The amount of the matrix and inverter-side inductor of the yield channel is displayed as L with a relating arrangement obstruction of R in order to have a bunch of straight powerful conditions for the three-stage framework associated PV framework.

$$L\frac{di_{gd}}{dt} = v_{id} - Ri_{gd} + \omega Li_{gq} - v_{gd} \tag{4.26}$$

$$L\frac{di_{gq}}{dt} = v_{iq} - Ri_{gq} + \omega Li_{gd} - v_{gq} \tag{4.27}$$

These are some essential equations of the dq frame. So, the dq frame rotating at angular speed $\omega$is represented in a form of matrix as:

$$\begin{bmatrix} v_{id} \\ v_{iq} \end{bmatrix} = R\begin{bmatrix} v_{id} \\ v_{iq} \end{bmatrix} + L\frac{d}{dt}\begin{bmatrix} i_{gd} \\ i_{gq} \end{bmatrix} + L\omega\begin{bmatrix} -i_{gq} \\ i_{gd} \end{bmatrix} + \begin{bmatrix} v_{gd} \\ v_{gq} \end{bmatrix} \tag{4.28}$$

The following equations can be obtained from

$$L\frac{di_{gd}}{dt} + Ri_{gd} = u_{idq} \tag{4.29}$$

$$v_{id} = u_{id} + v_{gd} - \omega Li_{gq} \tag{4.30}$$

$$v_{iq} = u_{iq} + v_{gq} - \omega L i_{gd} \quad (4.31)$$

The dq reference frame ensures the control of the power. The main goal is to either generate or receive sinusoidal currents.

The components are commonly used to control the active power on one side and the reactive power exchange on the other. The active I_{dref} and I_{qref} reactive power supplied to the grid can define as follow:

$$P_{dq} = \frac{3}{2}\left(v_d\, i_d + v_q\, i_q\right) \quad (4.32)$$

$$Q_{dq} = \frac{3}{2}\left(-v_d\, i_q + v_q\, i_d\right) \quad (4.33)$$

Where v_d , v_q , i_d and i_q represent respectively the direct and quadrature grid voltage currents components.

Therefore, equations and can be expressed as:

$$P_{dq} = \frac{3}{2}(v_d\, i_d) \quad (4.34)$$

$$Q_{dq} = -\frac{3}{2}\left(v_d\, i_q\right) \quad (4.35)$$

Then, the current can be deducing as follow:

$$i_d = \frac{2}{3} \times \frac{P}{v_d} \quad (4.36)$$

$$i_q = -\frac{2}{3} \times \frac{Q}{v_q} \quad (4.37)$$

From the input power, the inverter receives a DC power. S_1,S_2, S_3 and S_4 represents the gate of the MOSFET .and C_1 and C_2, the comparators of the PI controller. With the MOSFET that can turn on and off 120 times in a second. Comparators compare sine wave with triangular waves. The first one compares the normal sine wave and the second one the inverted sine wave. With the help of NOT gate at S_2 and S_4 in order to avoid having the four gates open at the same time. That configuration helps to reduce smooth voltage and limits the error.

Figure 4.4 presents the structure of the current control.

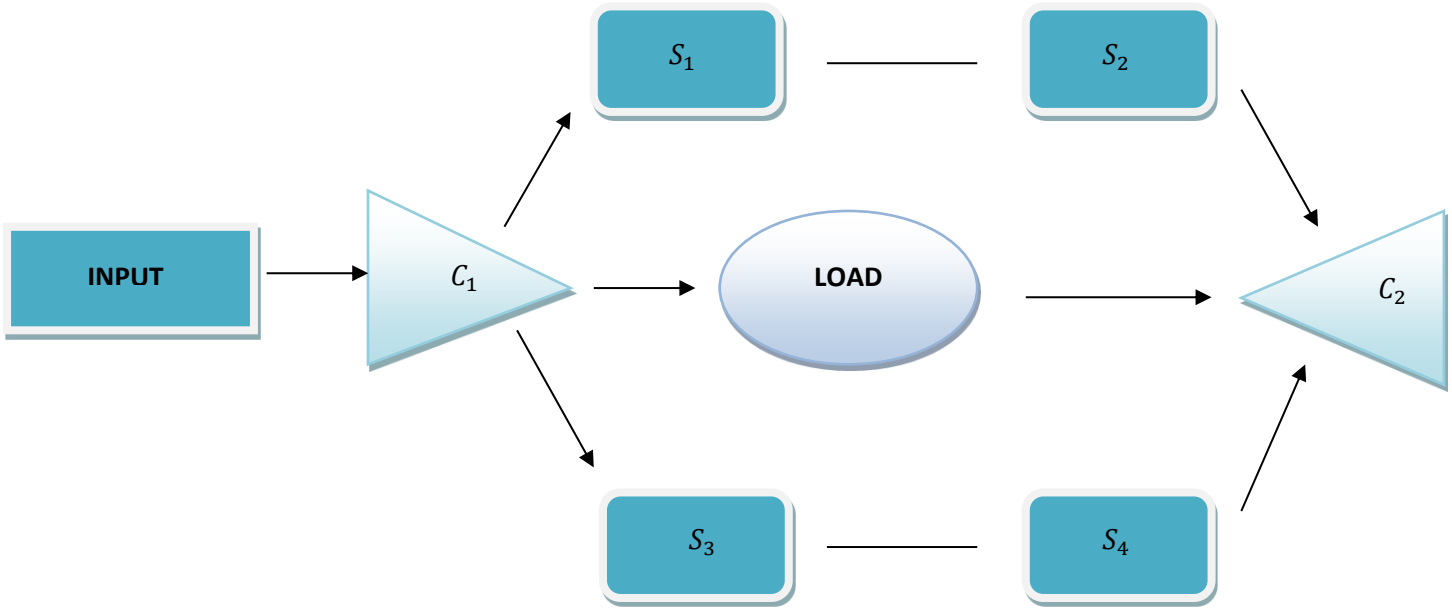

Figure 4.4: Current controller (Singh & Panigrahi, 2020)

4.5.2 Design of PI based Control scheme

The proposed PI controller is presented in Figure 4.5. It has been used for the simulations in this study.

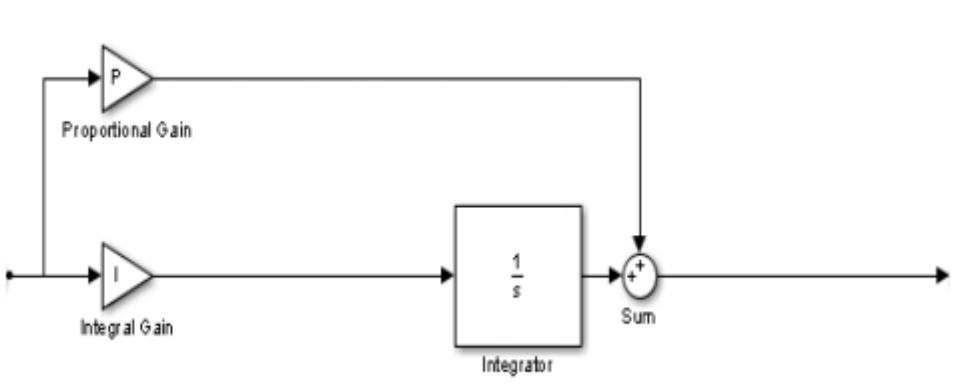

Figure 4.5: PI control loop (Badal & Das, 2019)

The PI controller is applied in order to allow the proper control of the voltage and regulates the MOSFET gates.

$K_p\ and\quad K_i$ are the proportional and integral gains and are respectively defined as:

$$G_{PI}(s) = K_p + \frac{K_i}{s} \tag{4.38}$$

$$= \frac{K_p s + K_i}{s} \tag{4.39}$$

And $G_D(s)$ represents the computation time delay

Where T_e is the control time delay

$$G_D(s) = \frac{1}{1+T_e} \tag{4.40}$$

Where $T_e = \frac{L}{R}$

Figure 4.6 represents the command structure used in the system.

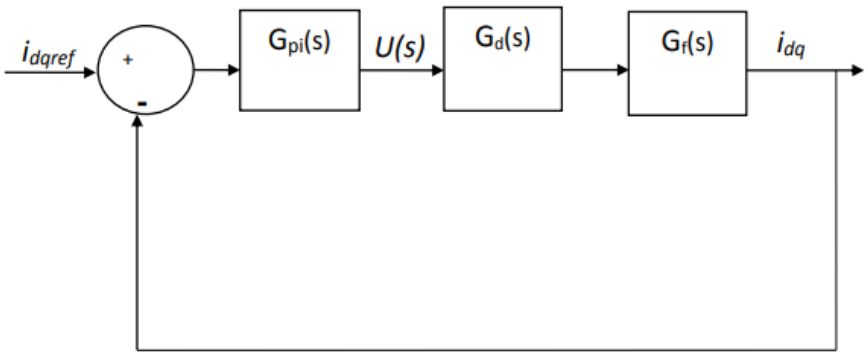

Figure 4.6: DQ reference command.

$$G_f(s) = \frac{v(s)}{i(s)} = \frac{1}{R+Ls} \tag{4.41}$$

$$G_f(s) = \frac{1}{R+Ls} \tag{4.42}$$

Where L = $L_i + L_g\ and\ R = R_i + R_g\ G_f(s) = \frac{241.5}{24.15+s}$
(4.43)

$$G_{oc}(s) = G_{PI}(s).G_d(s).G_f(s) \tag{4.44}$$

$$G_f(s) = \frac{K_p s + K_i}{s} \times \frac{1}{1+sT_e} \times \frac{1}{R+Ls} \tag{4.45}$$

$$G_f(s) = \frac{K_p s + K_i}{s} \times \frac{1}{1+sT_e} \times \frac{1/L}{R/L+Ls} \tag{4.46}$$

$$G_f(s) = \frac{K_p}{L} \times \frac{s + {K_i}/{K_p}}{s} \times \frac{1}{1+sT_e} \times \frac{1}{{R}/{L}+Ls} \quad (4.47)$$

$$\frac{K_i}{K_p} = \frac{R}{L} \quad (4.48)$$

After substituting into:

$$= \frac{K_p}{L} \times \frac{s + {R}/{L}}{s} \times \frac{1}{1+sT_e} \times \frac{1}{{R}/{L}+s} \quad (4.49)$$

$$= \frac{K_p}{L} \times \frac{1}{s} \times \frac{1}{1+sT_e} \quad (4.50)$$

$$G_{OC}(s) = \frac{K_p}{Ls^2T_e + s} = \frac{{K_p}/{L}}{s + s^2T_e} \quad (4.51)$$

Let k = $\frac{K_p}{L}$ (4.52)

$$G_{OC}(s) = \frac{k}{s^2T_e+s} \quad (4.53)$$

Then the closed loop current control is

$$G_{OC}(s) = \frac{G_{OC}(s)}{1+G_{OC}(s)} \quad (4.54)$$

$$G_{CC}(s) = \frac{\frac{k}{s^2T_e+s}}{1+\frac{k}{s^2T_e+s}} \quad (4.55)$$

$$G_{CC}(s) = \frac{k}{s^2T_e+s} \times \frac{s^2T_e+s}{s^2T_e+s+k} \quad (4.56)$$

$$G_{CC}(s) = \frac{k}{s^2T_e+s+k} \quad (4.57)$$

$$G_{CC}(s) = \frac{{k}/{T_e}}{s^2 + {s}/{T_e} + {k}/{T_e}} \quad (4.58)$$

The second order of the closed loop current control function is generally presented as follow;

$$G_{CC}(s) = \frac{\omega_n^2}{s^2+2\rho\omega_n^2 s+ \omega_n^2} \quad (4.59)$$

$$\omega_n^2 = \frac{k}{T_e} \quad (4.60)$$

$$\omega_n = \sqrt{\frac{k}{T_e}} \quad (4.61)$$

$$2\rho\omega_n = {1}/{T_e} \quad (4.62)$$

$$\omega_n = {1}/{2\rho T_e} \quad (4.63)$$

$$\sqrt{\frac{k}{T_e}} = {}^{1}/_{2\rho T_e} \quad (4.64)$$

Specifying $\rho \; to \; be \; {}^{1}/_{\sqrt{2}}$ and substituting $k = \frac{K_p}{L}$ back into equation

$$\sqrt{\frac{\frac{K_p}{L}}{T_e}} = \frac{1}{2\left({}^{1}/_{\sqrt{2}}\right)T_e} \quad (4.65)$$

$K_p = \frac{L}{2T_e}$(4.55)

$$K_p = \frac{L}{2T_e} \quad (4.66)$$

$= \frac{19.67}{2\times 0.01}$

$= 9.83$

$K_i = \frac{R\times K_p}{L}$

$= \frac{80\times 9.83}{19.67}$

$$K_p = 40$$

The value found above will help us to design the control system using the DQ theory in Simulink.

4.6 Summary

In this chapter, the design procedure and the control technique of the grid connected PV of 210kW has been studied. The LCL filter analysis and calculations were the core element of the study.But the grid connected inverter has an intermittent nature so there is a need for a proper control structure.

Chapter 5:

Simulation Results and Discussion

5.1 Introduction

5.2 Inverter output current and voltage

5.3 Voltage and current after the filter

5.4 Grid voltage and current

5.5 Active power injected to the grid

5.6 Reference and reactive current

5.7 Reactive power

5.8 System performance with step reference change in active and reactive power

5.9 Reactive power after the step reference change Iq

5.10 Conclusion

5.1 Introduction

This chapter presents and discusses the simluations results of the proposed system. The LCL filter represents the principal focus. From the findings; an approach of solution has been presented on how the harmonic in between the grid and inverter can be mitigated. The general structure of the system is presented in Figure 5.1.

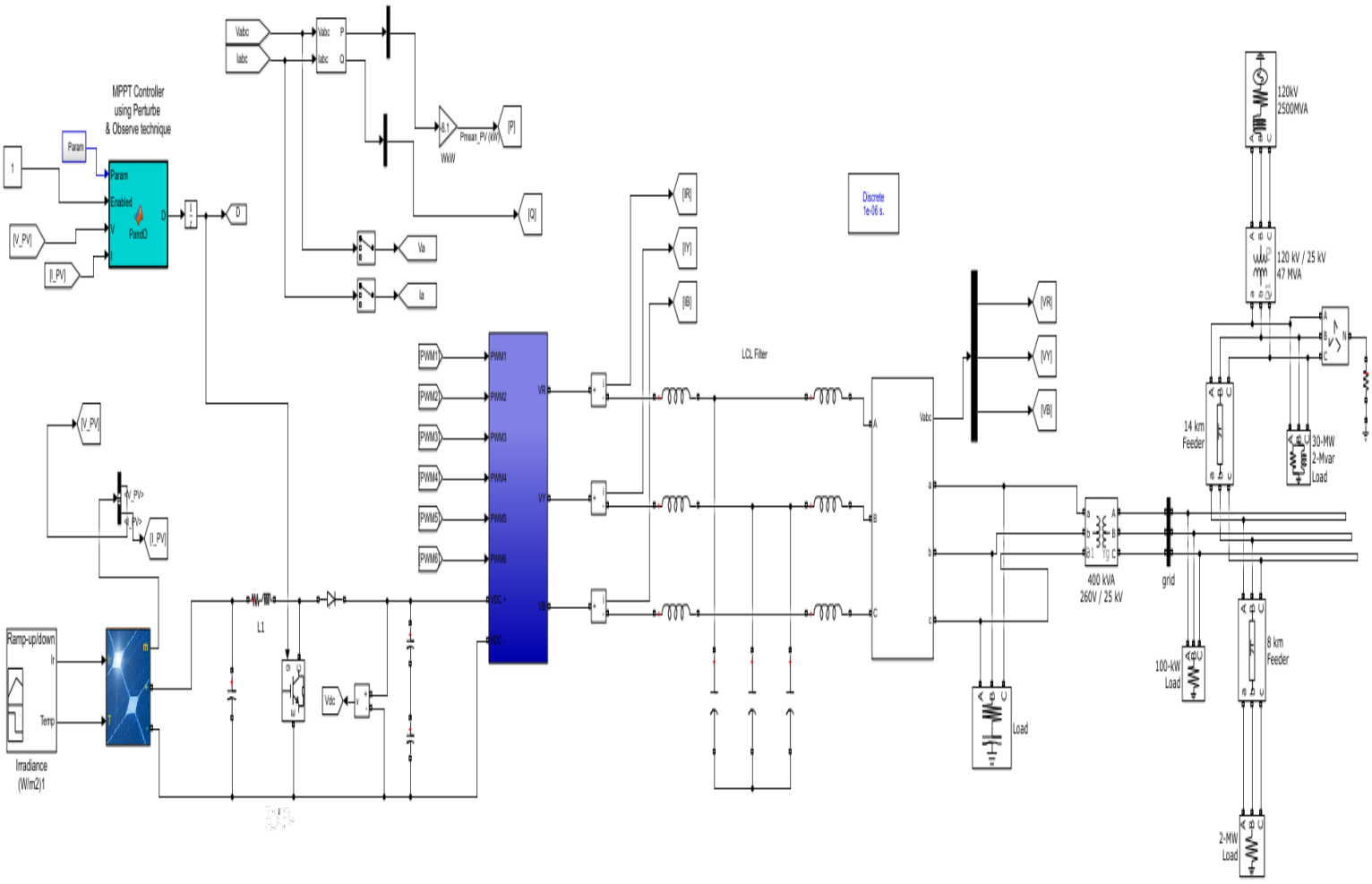

Figure 5.1 Three phase grid tied PV of 210kW

The figure 5.2 presents the inside block and the algorithm used for the MPPT

```
function D  = PandO(Param, Enabled, V, I)

% MPPT controller based on the Perturb & Observe algorithm.

% D output = Duty cycle of the boost converter (value between 0 and 1)
%
% Enabled input = 1 to enable the MPPT controller
% V input = PV array terminal voltage (V)
% I input = PV array current (A)
%
% Param input:
Dinit = Param(1);  %Initial value for D output
Dmax = Param(2);   %Maximum value for D
Dmin = Param(3);   %Minimum value for D
deltaD = Param(4); %Increment value used to increase/decrease the duty cycle D
% ( increasing D = decreasing Vref )
%

persistent Vold Pold Dold;

dataType = 'double';

if isempty(Vold)
    Vold=0;
    Pold=0;
    Dold=Dinit;
end
P= V*I;
dV= V - Vold;
dP= P - Pold;

if dP ~= 0 & Enabled ~=0
    if dP < 0
        if dV < 0
            D = Dold - deltaD;
        else
            D = Dold + deltaD;
        end
    else
        if dV < 0
            D = Dold + deltaD;
        else
            D = Dold - deltaD;
        end
```

Figure 5.2 MPPT algorithm

Based on the report of United States department of Energy analysis, a range of power of 210kW has been chosen. From the equations 4.6 and 4.7, the components this filter (inductance and capacitance) were determined. In Table 5.1, the parameters used to run the system are introduced

Table 5.1 : Parameters used for the system simulation

Parameter	Values	
PV power	240kW	
Inverter inductance	0.4mH	
Grid inductance	0.4mH	
Capacitance	15.35F	
DC link voltage	600V	
Grid	Phase to phase voltage	415V
	Frequency	50Hz
	Phase angle	0
Load	Active power	200kW
	Nominal frequency	50Hz
	Reactive power	100VAR

In (Moussavou, 2014), the author investigated the design of a PV system. From those analysis, it has been possible to replicate the same methodology according to this case. Table 5.2 shows the Specifications of a PV module that used in PV system of 210Kw

Table 5.2: Specifications of a PV module

Parameters	**Values**
Power (P)	250W
Parallel strings	57
Series connected per modules	15
Open circuit voltage (V_{oc})	37.8V
Voltage (V)	31.5V
Short circuit current (I_{sc})	8.7A
Current (I)	7.94A

Figure 5.3 represents the voltage output of the PV with a fixed temperature and irradiance.It showed the presence of oscillations. As in (Mustafa, 2017), the voltage shows those same ripples . The 600V as calculated were obtained from the output.

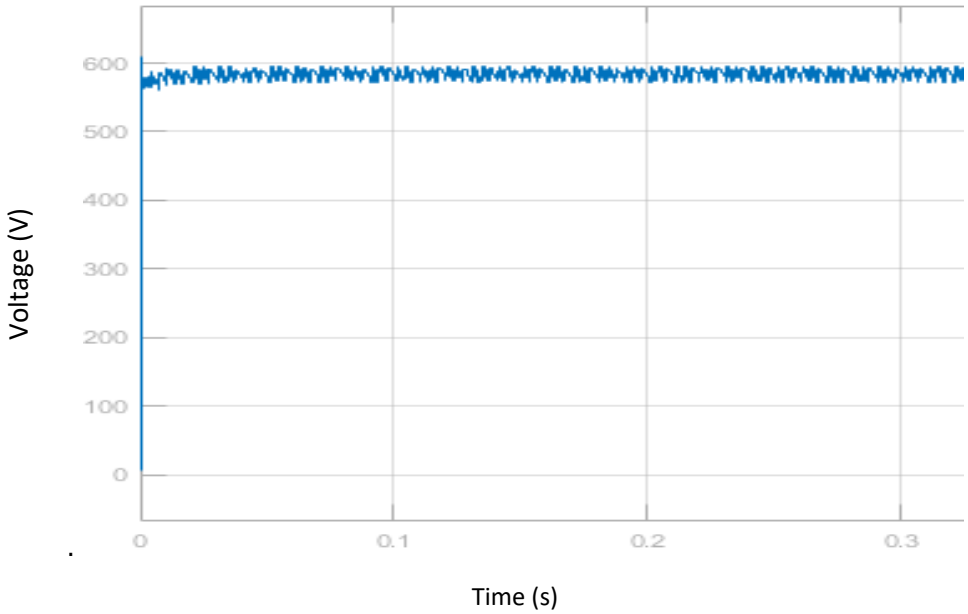

Figure 5.3: Voltage output of the PV

The irradiance variations from 1 to 10s are presented in figure 5.4. Figure 5.5 shows how the power varies regarding to the temperature and the iradiation. The power increased and reached its peak at 25 degree with a changing irradiance. From 1 second to 4, the irradiance was at 1000W/m^2 and a constant temperature of 25 degree, then the irradiance decreased to 600W/m^2 and same temperature which dropped the power to 120Kw.Last, the irradiance went back to 1000W/m^2 with 25 degree, the power wwnt back up to 210kw which is the desired maximum power point

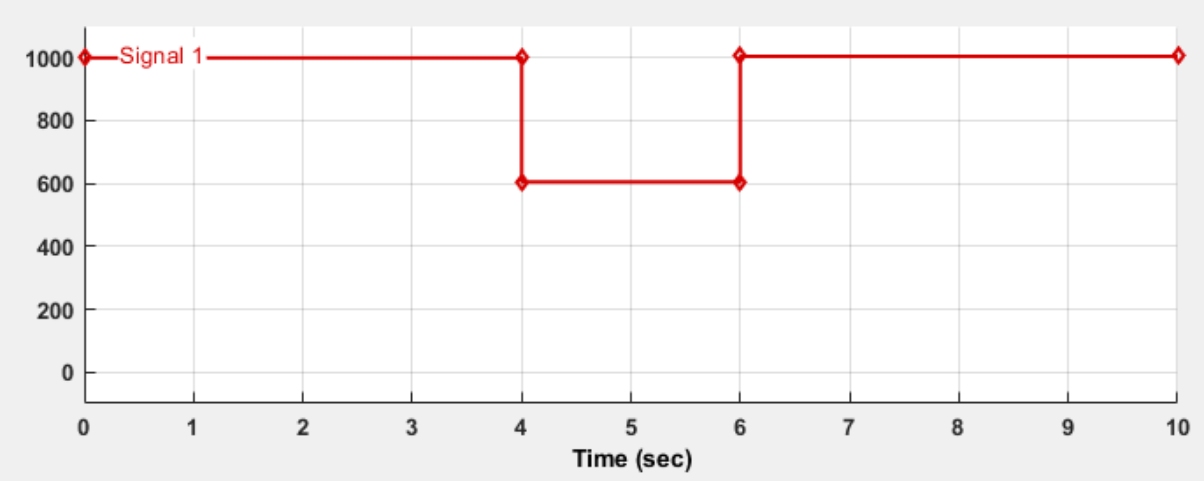

Figure 5.4: Irradiance variations

From the Figure 5.4, the Power generated from the PV system has been tracked. The power is equal to 210kW as predicted and only from 4s to 6s when the irradiande was pretty low the power decrease to 1.5kW

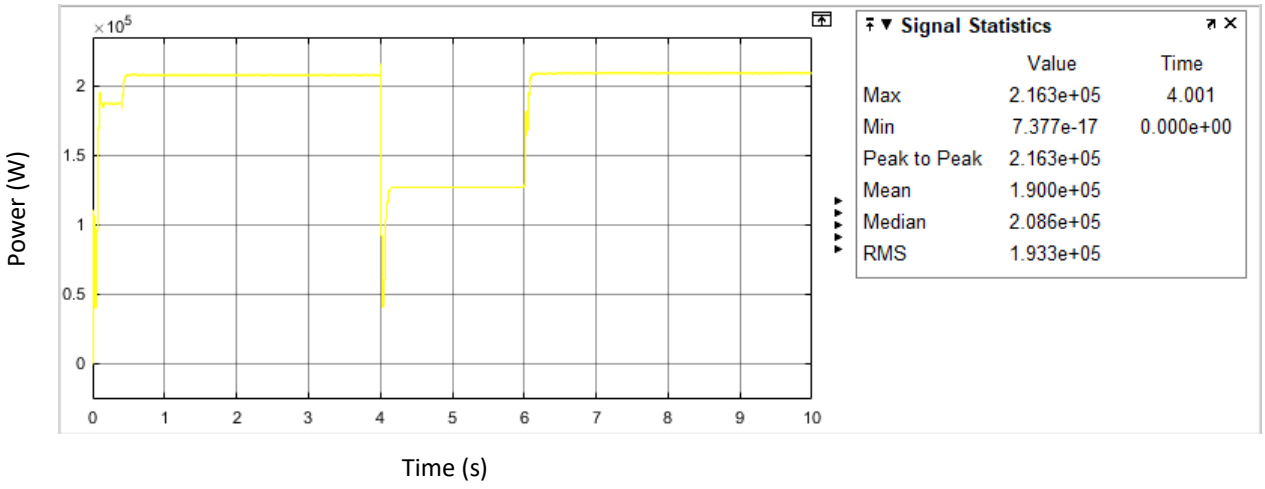

Figure 5.5: PV Power output

5.2 Inverter output current and voltage

Based on the table 4.3 in chapter four, the differents sequences of the inverter has been determined. With the equations (4.10,4.11and 4.12) that was studied in chapter four, a simulink model of three phase MOSFET inverter has been developed as seen in Figure 5.6 below.

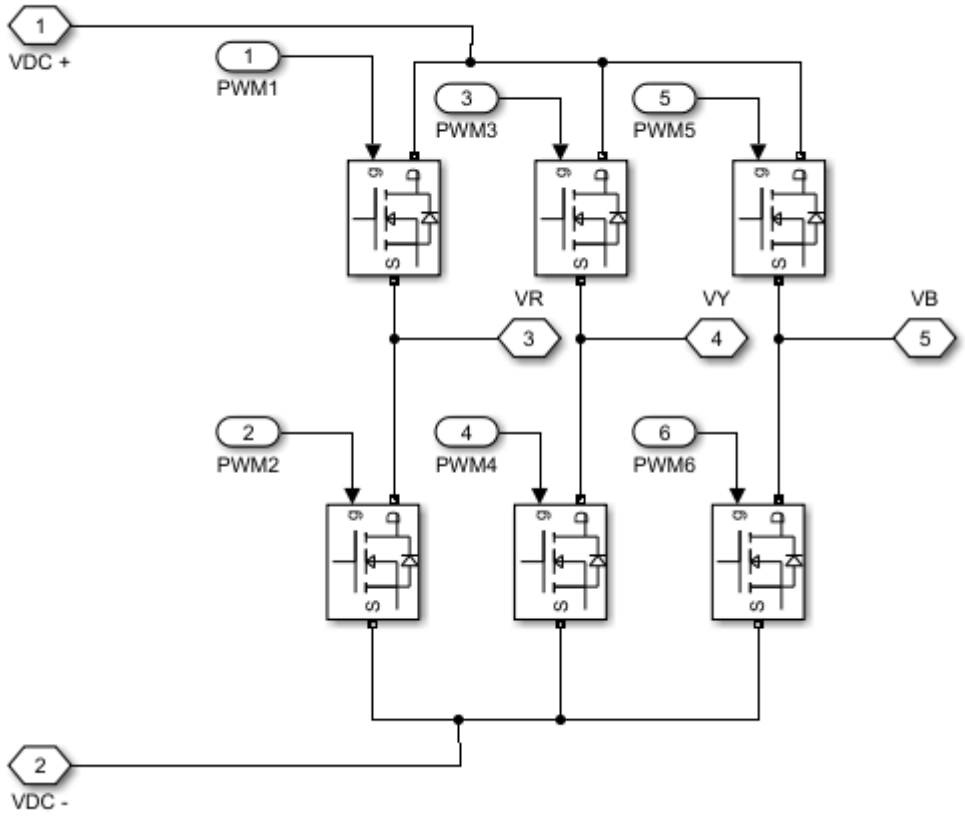

Figure 5.6: Three phase MOSFET inverter block

From Figure 5.7 with a pulse width modulation, the conversion of power from DC to AC has been made possible. It can be noticed some small ripples that confirm the presence of harmonics. The inverter output voltage changes between -600V and 600V. And the current varies from -150A to 150A.

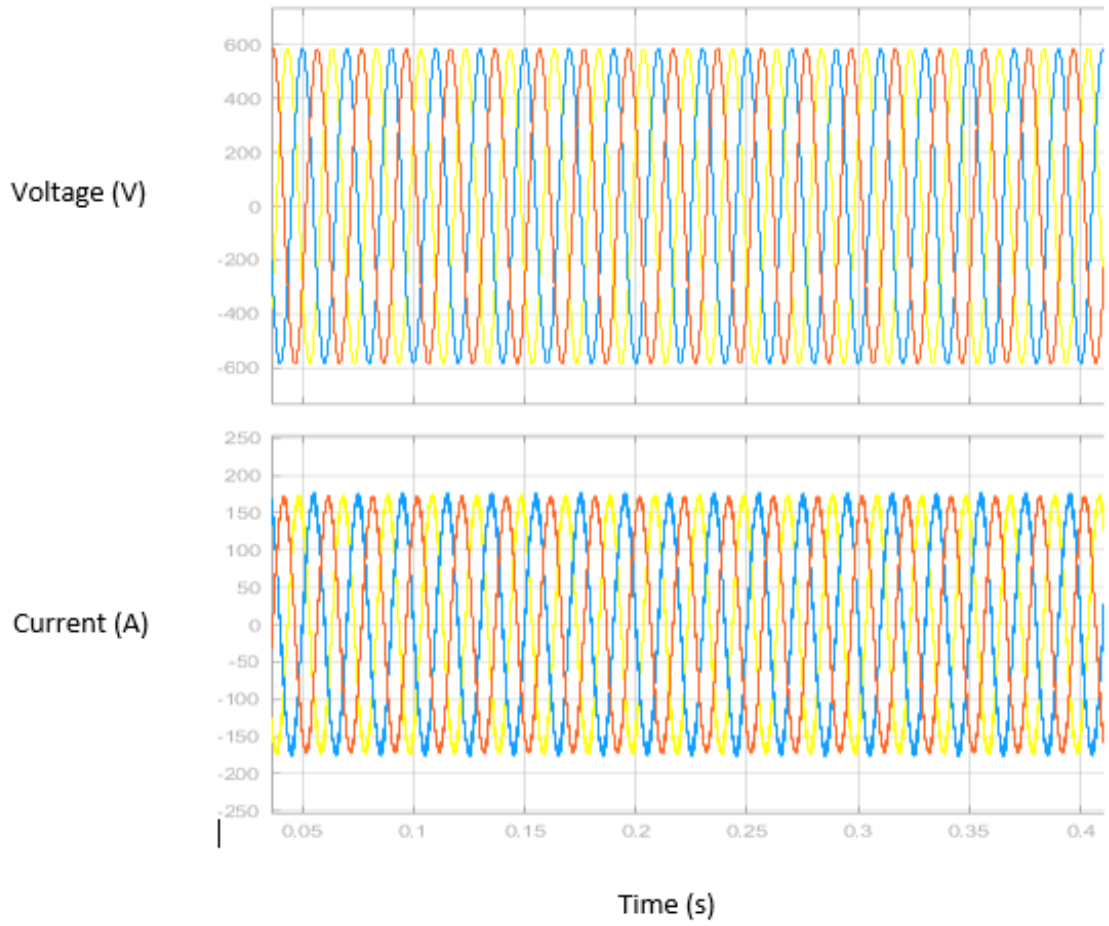

Figure 5.7: Three phase MOSFET inverter output.

The Figure 5.8 shows the Fast Fourier analysis of the system. A Total harmonic Distortion of 20.36% has been obtained which is a range of harmonic distortion regarding those types of system. And the objective is to reduce it fewer than 5% so that it matches the requirement of the IEEE519.

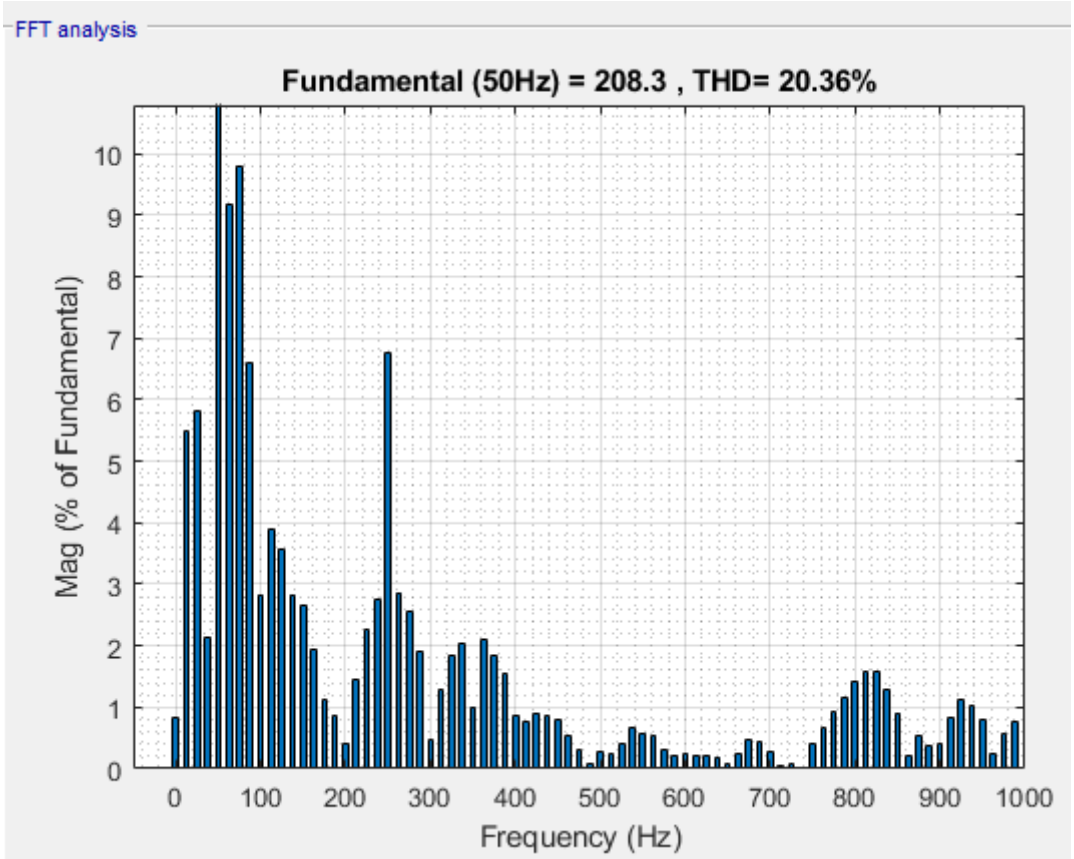

Figure 5.8: Fast Fourier Analysis

5.3 Voltage and Current after the filter

Once the LCL filter has been introduced, the voltage and current shows less ripples, in Figure 5.9 which demonstrate the absence of harmonics.

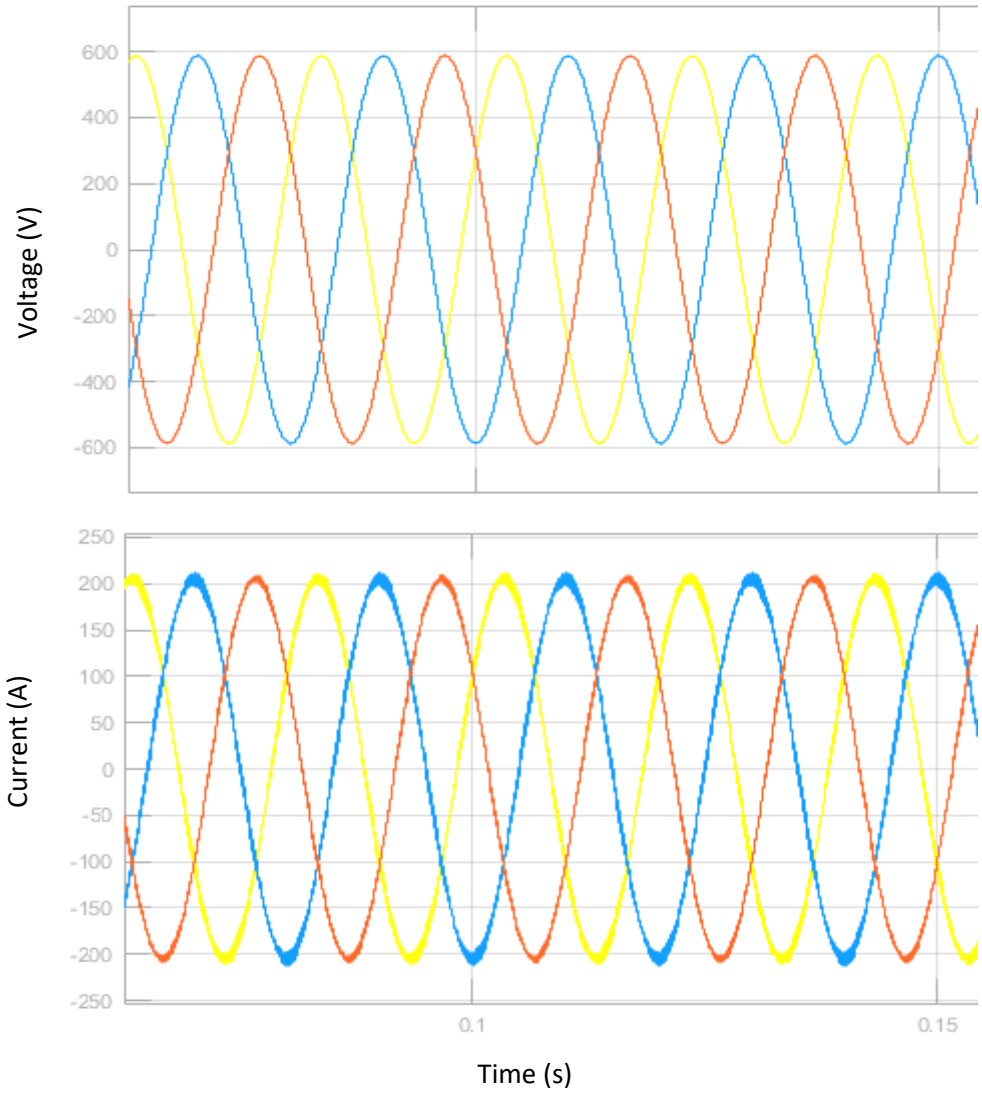

Figure 5.9: Voltage and Current with LCL Filter

5.4 Grid Voltage and current

The Phase voltage and line current at the grid-side are presented in Figure 5.10. The current lags behind the voltage by 90degree because of the nature of the inductor and how it opposes the change in the flow of the current itself.

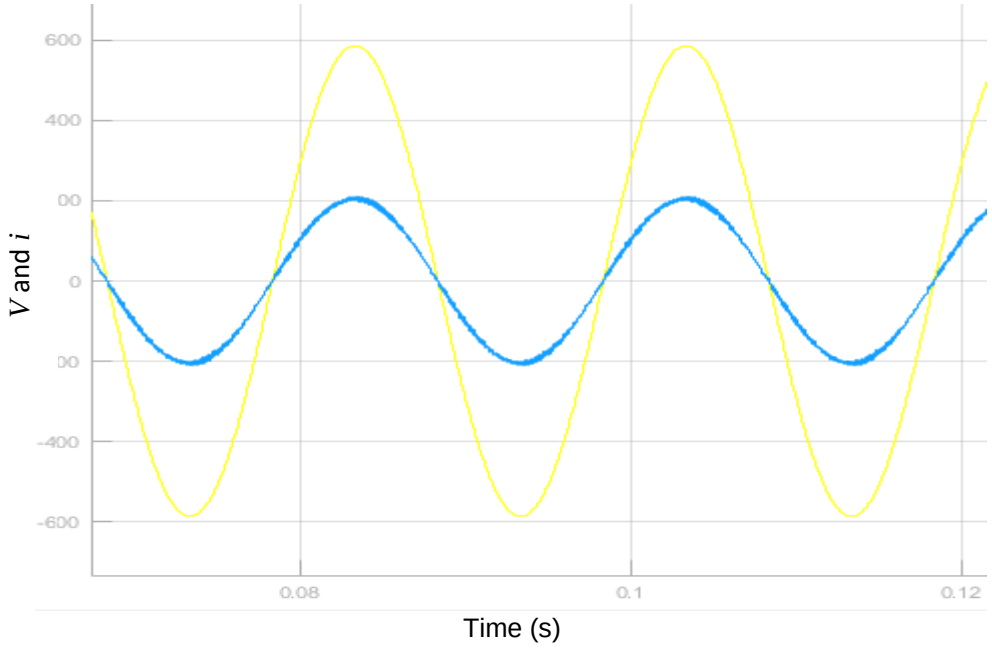

Figure 5.10: Grid voltage and current

Figure 5.11 depicted the Fast Fourier analysis allows us to observe the total harmonic distortion. The THD went from 25 to 2.39% with the introduction of the LCL filter which demonstrate its efficiency to perform when needed.

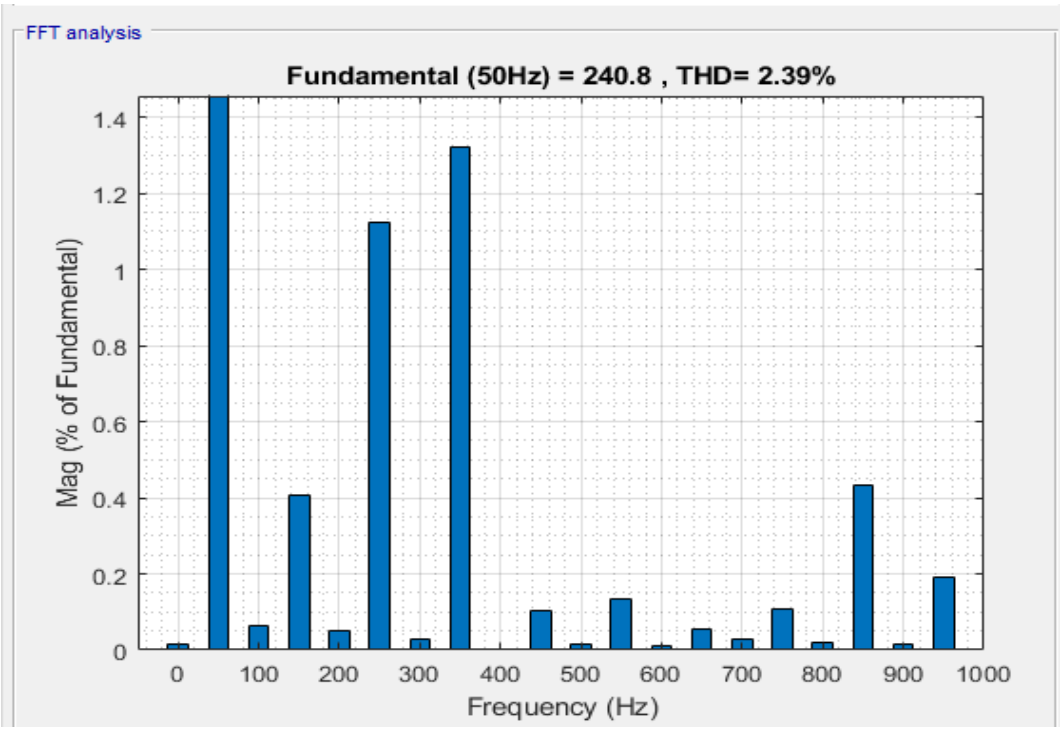

Figure 5.11: Fast Fourier Analysis after the filter.

5.5 Active power injected to the grid

The flow of active power that goes into the grid is displayed in Figure 5.12.The power is more or less 210kW which matches the predictions.

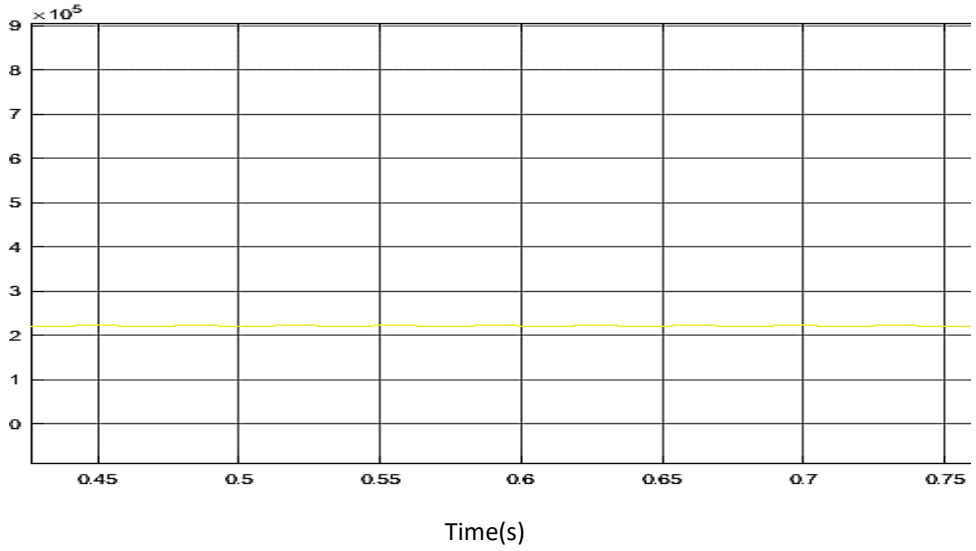

Figure 5.12: Active Power

In Figure 5.13, the d and q components of the modulating signals are presented. This was obtained from the equations resulting from the control strategy.

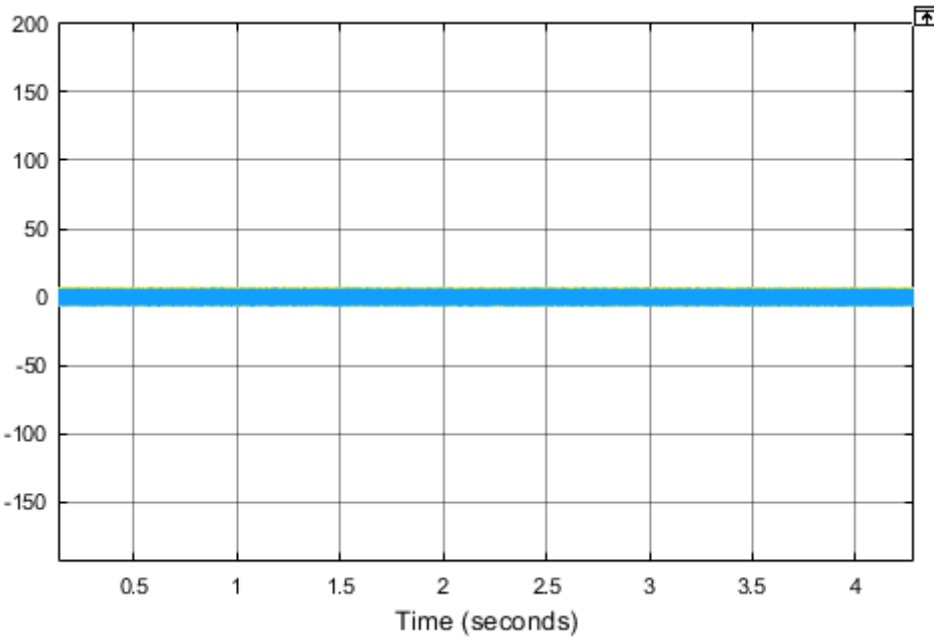

Figure 5.13: D and Q modulating signals.

5.6 Reference and reactive current (Iref, Iq)

The response from the q current component is plotted in Figure 5.14. There is a steady state of zero that demonstrates the ability of the tracking system.

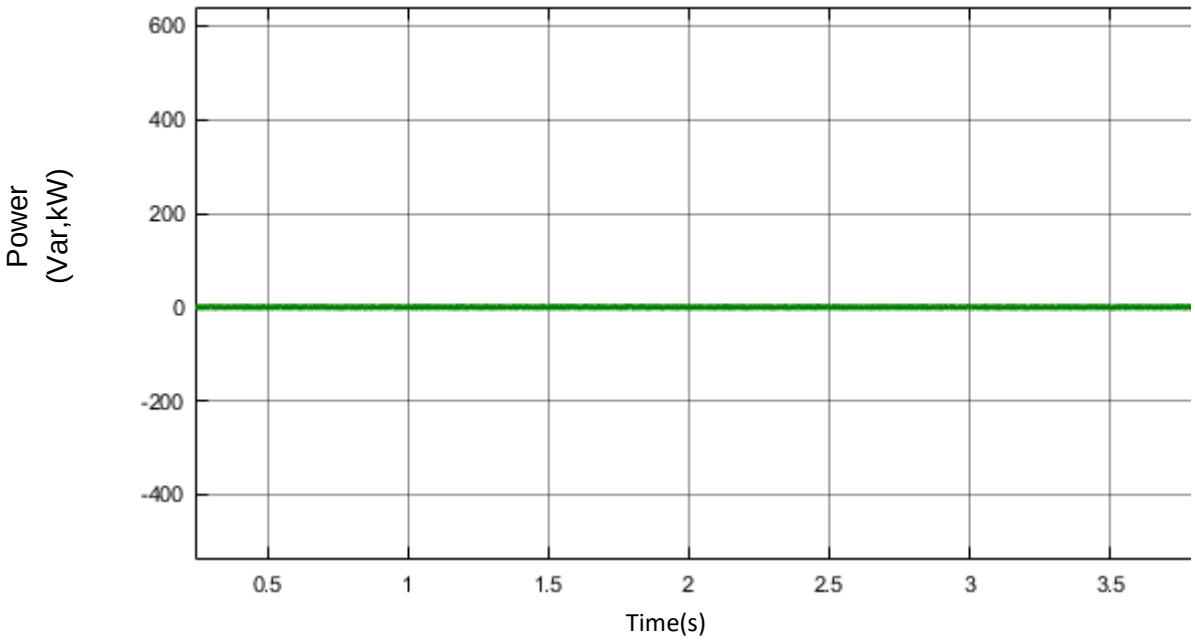

Figure 5.14: Active and reactive power reference

5.7 Reactive Power

The Figure 5.15 presents the reactive power injected into the grid. As predicted, it was not planned on sending reactive power to the network.

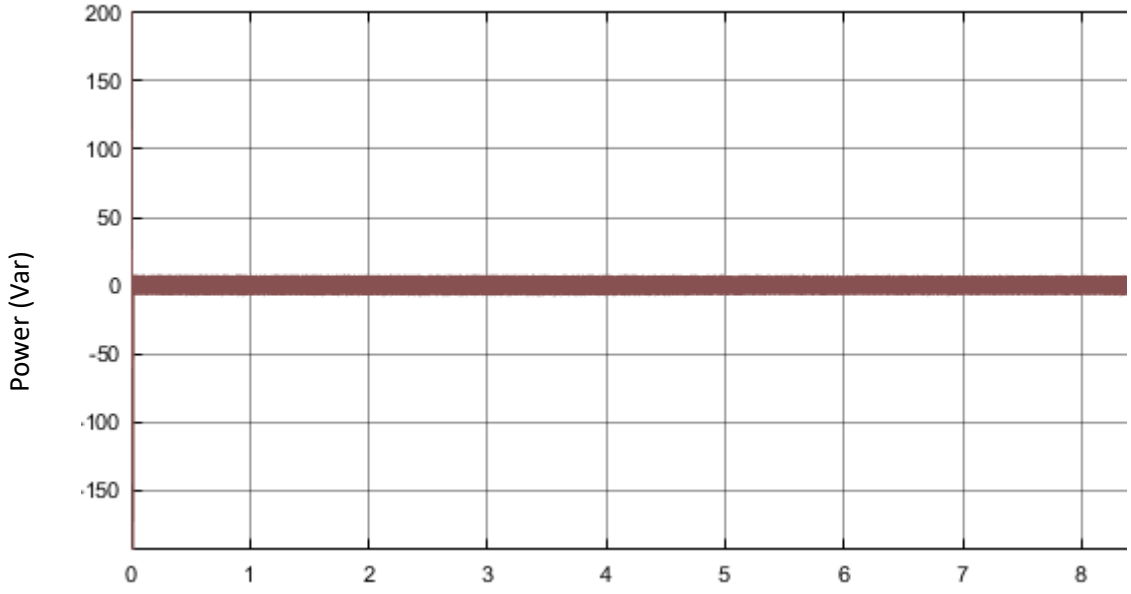

Figure 5.15: Reactive power output

5.8 System performance with step reference change in active and reactive power

From this scenario, changes have been made on purpose on Figure 5.5 on purpose. The next change operates when the active power increase from 210kW to 380Kw at 0.8 s and the reactive power also increases at this time as depicted in Figure 5.16 and 5.17. As some reactive has now been sent to grid.

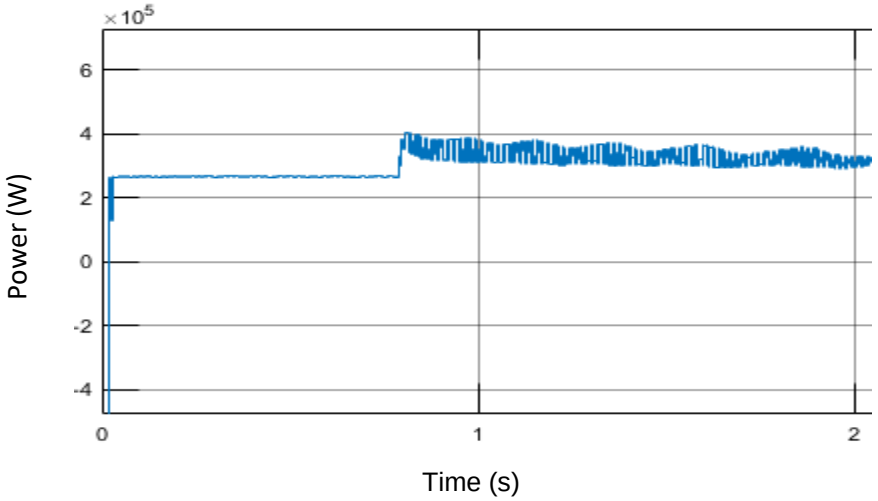

Figure 5.16: Active Power

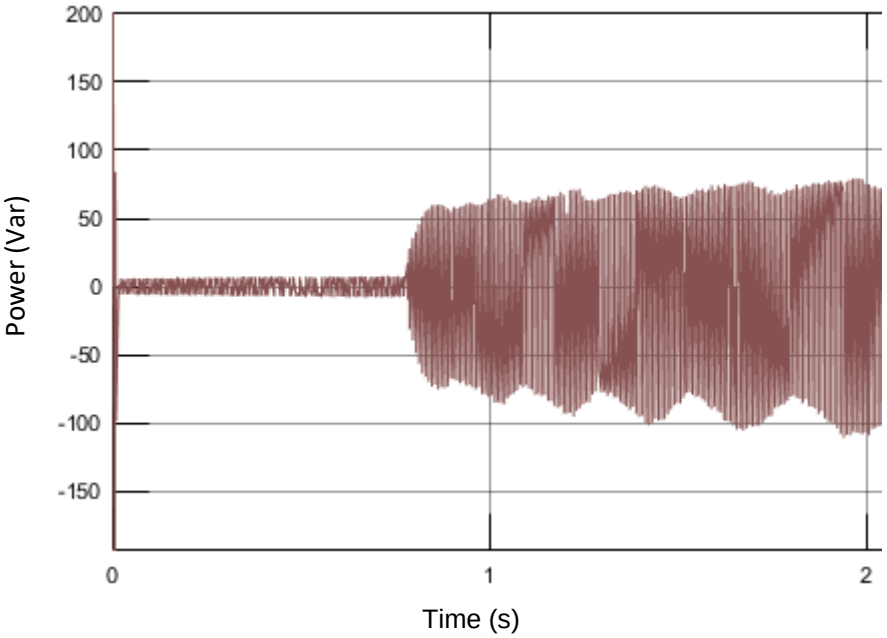

Figure 5.17: Reactive Power with step change

5.9 Reactive power after the step reference change Iq

A change of -200 on the current controller on Figure 5.1, in order to see if the total harmonic distortion is still low. The Figure 5.18 shows the voltage controlled with the dq theory and both sets to 0.

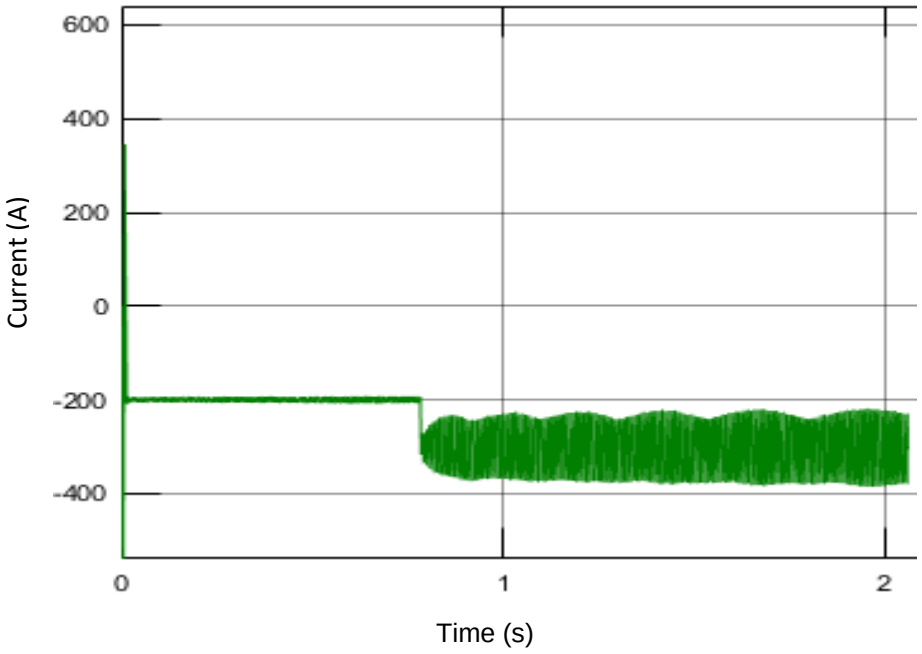

Figure 5.18: Step reference change with reactive power

The Figure 5.19 presents the Voltage after step reference change. The *dq* modulating signals display a value of zero which represents the error.

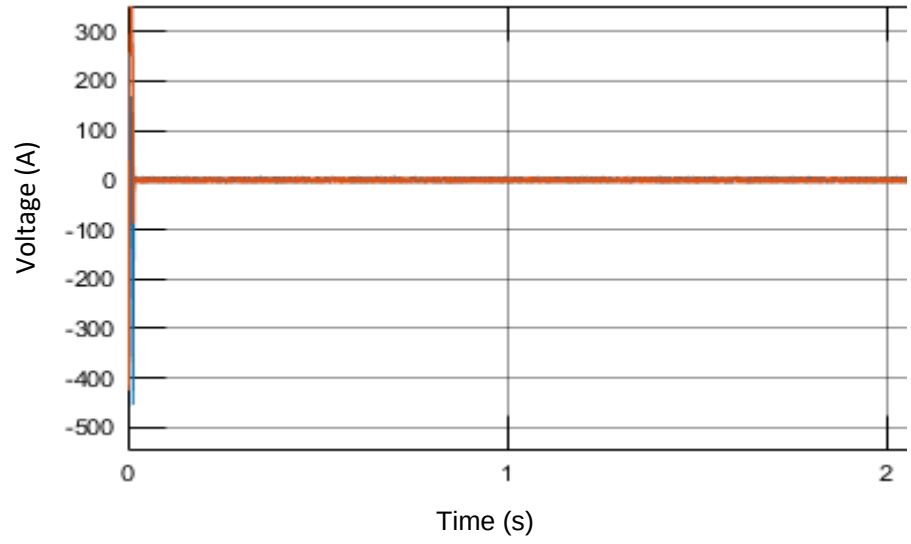

Figure 5.19: Voltage after step reference change

The response of both the current and the voltage after setting the reference points. The transition occurs at 0.8s; at this specific time the current went up from to 600A but the voltage remained constant as depicted in Figure 5.20.

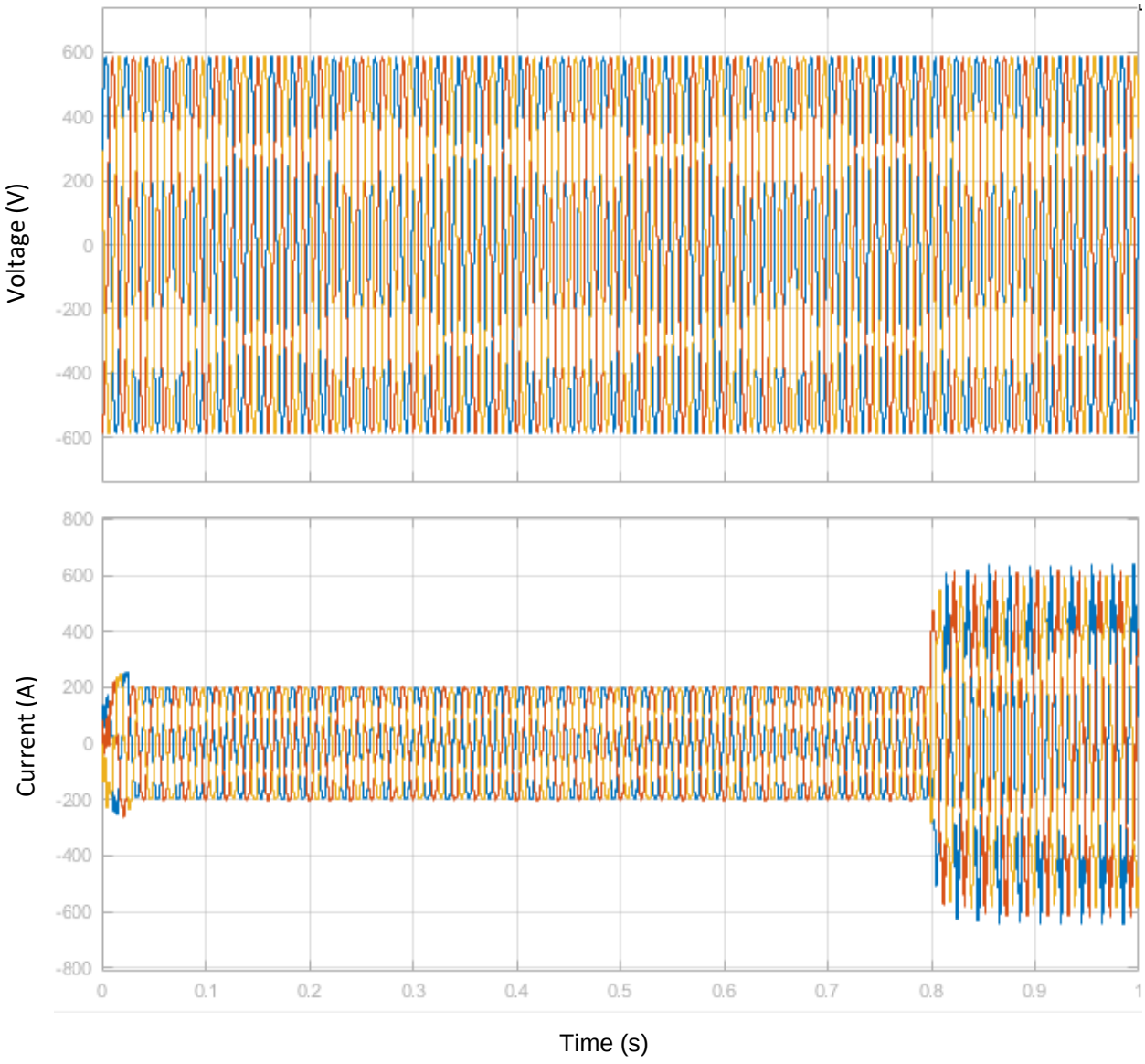

Figure 5.20: Current and Voltage after step reference change

Fast Fourier analysis after the filter still produce similar result as the previous one, the THD has been kept below 5%, to 2.5 % exactly which demonstrate that the LCL filter can work in different load and grid conditions as shown in Figure 5.21.

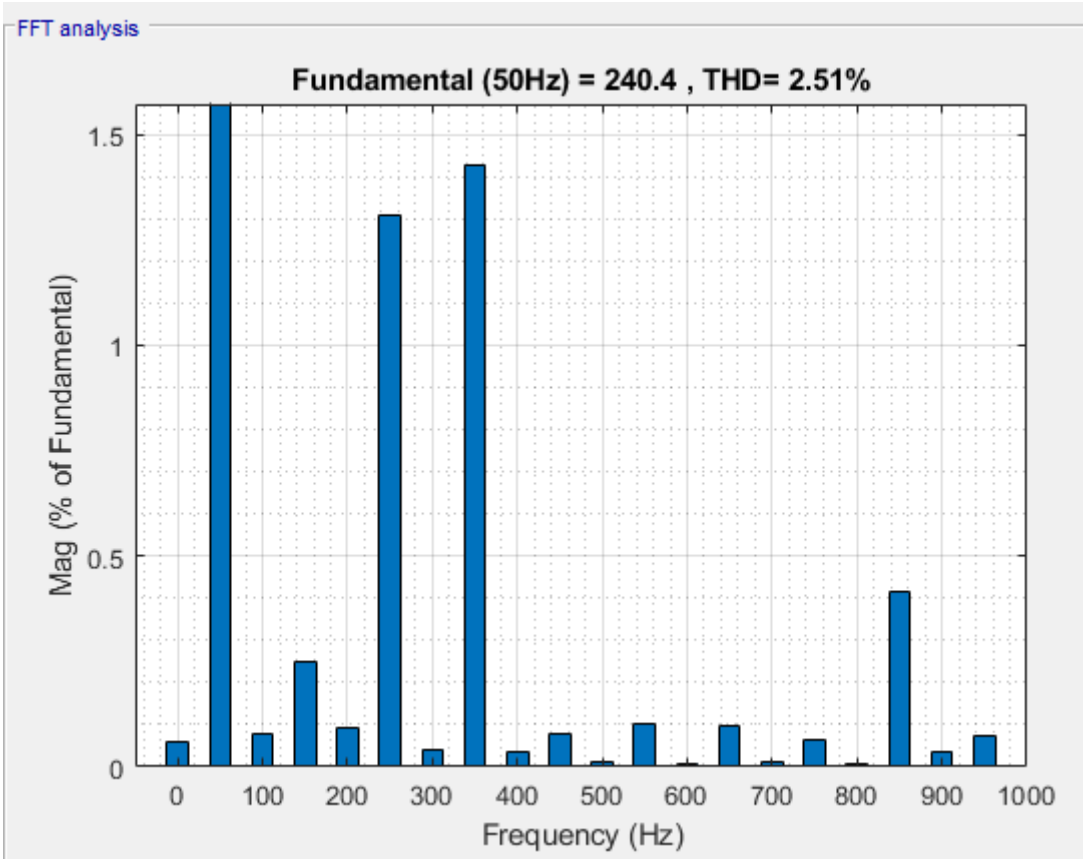

Figure 5.21 Total harmonic distortion after step change

5.10 Discussion

Two main scenarios have been introduced in the study, the first scenario consider an output power of 210kW and voltage of 600V. The level of harmonic revealed to be quite high and needed to be filtered. With the insertion of the LCL filter, the Harmonic level dropped significantly from 25% to 2.39%.In the second scenario , a step reference change is introduced the active power increased to 300kW and the reactive power to. Around 50 kVar .Still the designed filter perfectly mitigated the harmonics with a final level of 2.51%. All that comes to demonstrate how resilient and robust the designed filter is and his ability to be efficient besides the change of any conditions. Table presents the brief analysis of the filter impact

The table 5.3 presents the comparative analysis of the system

Table 5.3: Comparative analysis of the system

Comparative analysis	Before the filter	After the filter
THD scenario 1	20.36%	2.39%
THD scenario 2	20.36	2.51%

5.10 Summary

In this chapter, the LCL filter has been implemented into the three phase grid tied PV. First the system was run without filter, and a total harmonic distortion (THD) of 20.36% has been found. Once the filter implemented, the THD decreased to about 2%. And a second scenario has been tested where the active and reactive power were considerably increase, as expected the LCL filter has been able to keep the THD below 5% and then meet the IEEE519 standards.

The impact of the LCL filter on this grid connected system was analysed. Its effectiveness has been proven with the significant reduction of harmonic to which goes along with the IEEE 519 Standards.

Chapter 6: Conclusion and future work

6.1 Conclusion

6.2 Recommendations for future research

6.1 Summary

The comprehensive overview of renewable energy sources has been studied in the beginning of this thesis. The complete design of the LCL filter has been presented along with the other core components necessary to run the whole system such as the PV system, three phase MOSFET and current and voltage controller. The entire system has been modelled in MATLAB/Simulink.

In chapter two discussed the PV system in general, power quality and the filter topology. The grid connected PV system represents a core part of the system. A general description, operation mode and different types of topology are presented in order to provide an overview of different scenarios. And the final part of this chapter was particularly focused on the power quality. The harmonic impact on the grid was highlighted as well as the common types of filter used to mitigate its effects.

In chapter three, the mathematical description and all the related equations of each and any components of the three phase MOSFET inverter such as the PV, Boost converter , an overview of mathematical modelling of LCL filter have been explained. In order to have a clear overview of the elements that was used during the design of the system

In chapter four ,the design procedure and the control technique of the grid connected PV of 210kW has been studied. The LCL filter analysis and calculations were the core element of the study. Several factors influence the design of a LCL Filter such as: cost effectiveness, attenuation and harmonic elimination potential. The design started from the derivation of the transfer function of the LCL function from the mathematical model developed in chapter three. The following parameters have been used during the calculations the line to line Voltage, Grid frequency, Nominal Power and Current. Then after the calculation process, the LCL filter has a grid side inductor and inverter respectively of 8.67 mH and 10.91mH a capacitance of $23.1\mu F$.With a damping resistor of which can effectively absorb the higher harmonic contained in the system.

The inverter used in this study is a three phase DC to AC with PWM technique. The bidirectional ability of this system is crucial because it allows the processing of the power from the load to the grid and vice versa. Then a six switches stages system is introduced. The lower and upper parallel branch of the inverter receives the DC power. The Mosfet switches have preferred as it widely used in such configuration. The dq synchronous reference is applied in order to decrease the mathematical model dimension and facilitate the control process. Basically, with the PLL, the tracking of another system is easier. The proportional integral controller and the PLL supply the signal and then contribute to stabilizing the frequency

between the grid and the source. With the proportional integral controller brings the error percentage to zero and the PLL deals with the fluctuations of the frequency.

With a current controller, the instability can be solved when planning the GCI. And it provides more security for the inverter. Due to the current control framework, the VSI isn't at chance of over .But the grid connected inverter has an intermittent nature so there is a need for a proper control structure

In chapter five, the impact of the LCL filter on this grid connected system was analysed. The design developed previously has been in implemented in MATLAB/Simulink. A 210kW PV system with Mosfet inverter that supplies power to the grid. In the First scenario, the system is runned with 600V voltage and current that both presented ripples and a high harmonic presence. Once the LCL filter has been introduced both ripples and total harmonic distortion has decreased significantly. With a grid voltage and current in phase, it demonstrate that the system work perfectly.

In the Second scenario, a step change on the power has been applied, it went from 210kW to 300kW, and has for impact to influence the reactive power as well. With the PI controller the power has been pushed in such an undesirable reactive power, besides that at the end of the running with the same filter. It still able to mitigate and maintain the harmonic below a certain level which is 2 %.

The effectiveness of the designed filter has been proven with the significant reduction of harmonic from 20 to which goes along with the IEEE 519 Standards.

6.2 Recommendations for future research

With the growing need in energy and renewable energy sources expansion, inverters will play a significant role. From what have been developed in this research several other aspects can be included in the future research:

- Comparative analysis with different filter topology and introducing efficiency and cost analysis in order to draw the most cost effective.
- Experimental setup
- Expand and develop more on the control strategy and the inverter operation
- Communication interface introduction

References

Abbadi, A., Hamiddia, F. & Morsli, A., 2018. *New MPPT Sliding Mode Approach for Grid Connected PV System.* s.l., IEEE Transactions on Smart Grid, pp. 36-42.

Abdelbasset, K., Reffat, S. & Trabelsi, M., 2019. *Model Predictive Control of a 9 level Packed U cells based grid connected PV system.* s.l., IEEE Transactions on Smart grid, pp. 87-93.

Abujubbeh, M. & Marazanye, V., 2019. *Techno Economic Feasability Analysis of Grid Tied PV Wind hybrid system to meet a typical household demand: Casa Study Amman ,Jordan.* s.l., IEEE Transacrion on Global Power, Energy and Communication Centre, pp. 6-9.

Ayalew, B., Afolabi, A. & AL Dura, A., 2020. *Robust Continuous Nonlinear Predictive Controller via Integral Sliding Mode Control for Grid Tied PV Inverter.* s.l., IEEE Transactions on Smar Grid, pp. 66-72.

Ayalew, B., Afolabi, A. & Al Durra, A., 2020. *Robust Continuous Nonlinear Predictive Controller via Integral Sliding Mode Control for Grid Tied PV Inverter.* s.l., IEEE Transactions on Smart Grid, pp. 556-557.

Badal, F. & Das, P., 2019. *A survey on control issues in renewable energy intergration and microgrid,* s.l.: IEEE Transactions on Power system.

Battacharya, S. & Kumar, S., 2019. *Adaptative Damped Circular Current Limit Control for PV Grid Tied System.* s.l., IEEE Transactions on Power System, pp. 14-19.

Burlaka, V., Gulakov, S. & Podnebennaya, S., 2019. *Low Cost Transformeless Grid Tie Inverter For Photovoltaic System.* s.l., IEEE Transactions on Smart Grid.

Chandra, K. & Kulkarni, P., 2020. *Desing and Performance evaluation of Proposed 2kW Solar PV Rooftop on grid system in Odisha using PVsyst.* s.l., IEEE Transactions on Power System, pp. 8-9.

Chen, T., Rahim, A., Peng, F. & Wang, H., 2019. *An improved Finite Control Set MPC Based Power Sharing Control Strategy for Islanded AC Microgrids.* s.l., IEEE Transactions on Microgrids, pp. 54-57.

Chishti, F., Singh, B. & Murshid, S., 2020. PCC Voltage Restoration strategy of an isolated microgrid based on adjustable step adaptive control. *IEEE Transactions on Industrial Application,* 56(6), pp. 32-38.

Dhaneria, A., 2020. *Grid Connected PV System with Reactive Power Compensation for the Grid.* s.l., IEEE Transactions on Power System, pp. 6-7.

Dhaneria, A., 2020. *Grid connected system with greactive power compensation for the grid.* s.l., IEEE Transactions on Power systems, pp. 85-90.

Driesen.J, S., 2013. *Optimal analytic LCL filter design for grid-connected voltage-source converter.* Zagreb,Crotia, IEEE.

Dutta, S. & Chatterjee, K., 2018. A buck and boost based Grid connected PV Inverter Maximizing Power Yield from two PV Arrays in Mismatched Environmental Conditions. 65(7), pp. 43-50.

Elmelegi, A., Aly, M. & Alhaider, M., 2019. *An Efficient Low< Cost Distributed MPPT Method gor Energy Harvesting in grid tied three phase PV power optimizers.* s.l., IEEE Transactions on Power system, pp. 9-11.

Errouissi, R. & Al Durra, A., 2019. Disturbance Observed Based Control Photovoltaic System Under Unbalanced Grid Voltages. *IEEE Transactions on industrial Electronics,* 66(11), pp. 18-19.

Errouissi, R. & AL Durra, A., 2019. *Disturbance Observer Based Control for Dual Stage Grid Tied Photovoltaic System Under Unbalance Grid Voltages.* s.l., IEEE Transactions on industrial Electronics, pp. 58-63.

Fajri, D., Winanti, N., Purwadi, A. & Heryana, N., 2018. *Performance Evaluation of 1.8kWp Grid Tied PV system art Al Umanaa BOarding School.* s.l., IEEE Transactions on Power systems, pp. 84-89.

Geetha, A. & Subramani, C., 2018. *study of LCL filter performance for inverter fed grid.* Chenai;India, IEEE Transactions on Power Electronics, pp. 1-5.

Gong, C., Ji, H., Chen, H. & Li, X., 2019. *Research on Distributed Control Strategy based on Hierarchical Control of Microgrid.* s.l., IEEE Transactions on Microgrid, pp. 57-63.

Hanif.M&Jalayath.S, 2016. *Generalized LCL-Filter Design Algorithm for Grid-Connected Voltage-Source Inverter.* s.l., IEEE.

Han, Y., Ning, X. & Yang, P., 2019. *Review of power sharing, voltage restoration and stabilization techniques in hierarchical controlled DC microgrids.* s.l., IEEE Transaction on Power System, pp. 14903-14923.

Hinsui, T. & Sangtuntong, W., 2019. *Voltage Observer Based Control for Single Phase Grid Connected PV Inverter.* s.l., IEEE Transaction on Control System, pp. 4-6.

Hornik.T & Zhang.Q, 2011. A Current-Control Strategy for Voltage-Source. *IEEE Transactions on Power Electronics,* March.26(3).

Inci, M., 2019. *Design and Analysis of Dual Level Boost Converter Based Transformeless Grid connected PV system for Residential Applications.* s.l., IEEE Transactions on Power Electronics, pp. 91-98.

Islam, S., Zeb, K., Uddin, W. & Khan, I., 2019. *Design and Investigation of FRT Schemes for three phase Grid Tied PV System.* s.l., IEEE Transactions on Power System, pp. 9-11.

Jadhav, R. & Patil, S., 2020. *Design and Implementation of PV Wind Battery Hybrid System for OFF Grid and On Grid.* s.l., IEEE Transactions on Control systms, pp. 6-9.

Jain, V. & Signh, B., 2019. *Power Quality Improvement in PV System Tied to Weak Grid.* s.l., IEEE Transactions on Power Systems , pp. 9-14.

Jain, V. & Singh, B., 2020. *An IGI FLL Controlled PV system with Power Filtering Capabilities under Distorted Grid Conditions.* s.l., IEEE Transacations on Smart grid, pp. 6-11.

Jain, V. & Singh, B., 2020. *An IGI FLL Controlled PV System with Power Filtering Capabilities under Distorted Grid Conditions.* s.l., IEEE Transactions on Smart Grid, pp. 66-72.

Jian, Z., Fang, L., Weijun, Z. & Yi, Z., 2019. *Simulation of PV grid connected Inverter based on FSCAD.* s.l., IEEE Transactions on Smart Grid.

Jiao, J., Meng, R., Wang, L. & Zhang, B., 2019. *Grid Connected Control Strategy for Bidirectionnal AC to DC Interlinking Converter in AC DC Microgrid.* s.l., IEEE Transactions on Industrial applications, pp. 1-9.

Kakkattukunnumal, J., Das, N. & Palmer, E., 2019. *Techno Economic Performance Analysis of Grid Tied and Standalone PV System in Victoria.* s.l., IEEE Transactions on Power System, pp. 3-8.

Kanagatakshmi, S., Mageshwari, S. & Kumar, A., 2019. *Design of Control Strategy of DC/AC Converter fro Grid Connected PV system.* s.l., s.n., pp. 1-19.

Kan, Z. et al., 2020. *Research on Grid Connected/Islanded Control Strategy of PV and Battery Storage system as Emergenecy power supply.* s.l., IEEE Transactions on Power System.

Kapil.N & Rushiraj.G, 2016. *Analysis of different modulation techniques for multilevel inverters.* Delhi,India, IEEE.

Keddar, M., Doumba, M., Krachai, L. & Belmokthar, K., 2019. A new energy management strategy of an autonomous microgrid based on virtual impedance in multilevel droop control inverters. *International Journal of Computer and Electrical Engineering,* June, 5(3), pp. 322-325.

Kimaiyo, K. B., Sirisamphawong, C. & Somkun, S., 2019. *Effect of Voltage Unbalance on the Power Quality of Three Phase Grid Connected PV Inverters.* s.l., IEEE Transactions on Power System, pp. 61-67.

Kishor, P., Panda, K. & Panda, G., 2021. Current Reference Control Based MPPT and Investigation of Power Management Algorithm for Grid Tied Solar PV System. *IEEE System Journal,* pp. 31-39.

Kolte, P. & Mohale, V., 2019. *Improved System of Constant Power Generation in Grid Connected PV Cell with Battery.* s.l., IEEE Transactions on Power System, pp. 61-68.

Kumar.J, Agarwal.A & Agarwal.V, 2019. A review on overall control of DC microgrids. *Journal of Energy Storage,* pp. 117-138.

Kumar, A. & Singh, B., 2019. *Multifunctional Grid Tied PV System Using Modified KLMS Control.* s.l., IEEE Transactions on Power Systems, pp. 6-9.

l.molino, 2014. Power Control and Management in a Hybrid AC/DC Microgrid. *IEEE Transaction on smart grid,* May.5(3).

Li, H., Zhang, X. & Wan, T., 2019. *Small Signal Stability analysis of PV Grid connecetd system under weak grid conditions.* s.l., IEEE Transactions on Power System, pp. 61-69.

Li, J. & Li., 2020. *Improved Current based Droop Control strategy for microgrid Inverters.* s.l., IEEE Transactions on power electronics, pp. 1070-1075.

Li, Y. et al., 2020. *Autonomous Control Strategy for Microgrids Opeartions modes.* s.l., IEEE Transactions on Power System, pp. 56-61.

Loka, R. & Parimi, R., 2020. Impact of Microgrid Connected to a Conventional Power System on System Frequency and Control Strategy. *IEEE Transactions ,* September, 10(9), pp. 5067-5077.

Lopez.I, et al., 2016. Modulation Strategy for Multiphase. *IEEE Transactions on Power Electronics,* February.31(2).

Mao.L, Y., 2018. *An overview of a photovoltaic system.* Shenyang,China, IEEE.

Matiyali, K., Goel, S. & Joshi, H., 2019. *Voltage Oriented Control of Grid Tied Solar PV System.* s.l., IEEE Transaction on PowerSystem, pp. 9-13.

Mazaheri, A., Barati, F. & Ghavipanjeh, F., 2019. *Multi Variable PI Control Design for Grid Tied Three Phase PV Inverters.* s.l., IEEE Transactions on power Systems, pp. 5-14.

Mazaheri, A., Barati, F. & Ghavipanjeh, F., 2019. *Multivariable PI Control design for Grid Tied Three Phase PV Inverters.* s.l., IEEE Transactions on Renewable Energy, pp. 36-46.

Mehiri, A., Kadir, A. & Almazrouie, S., 2017. *The Effect of Shading with Different PV Array Configurations on the Grid Connected PV System.* s.l., IEE Transactions on Smart Grid, pp. 6-9.

Moftah, M. A., Saady, G. e. & EL-Noby.A.Ibrahim, 2016. Active power filter for power quality enhancement of photovoltaic renewable energy systems. *IEEE.*

Mohapatra, S., Agarwal, V. & Patawardhan, S., 2020. *Experimental Evaluation ofInternal Model Control for 3 phase grid tied Spolar PV Inverter.* s.l., IEEE Transactions on Smart Grid, pp. 6-9.

Monge.S, Martinez.A & Alepuz.S, 2017. A Modulation Strategy to Operate Multilevel Multiphase Diode-Clamped and Active-Clamped DC–AC Converters at Low Frequency Modulation Indices With DC-Link Capacitor Voltage Balance. *IEEE Transaction on Power Electronics ,* 32(10), pp. 7521 - 7533.

Mostefaoui, M., Sahouane, N., Dabou, R. & Ziane, R., 2018. *Importance Cleaning of PV modules for grid connected system in desert environment.* s.l., IEEE Transaction on Power System, pp. 53-58.

Mukeerjee, S. et al., 2019. *Performance of Fed Grid Connected Inverter Fed from PV Array.* s.l., IEEE Transactions on Power System, pp. 36-39.

Narendra, A., Ventkataramana, N., Panda, A. & Tiwary, N., 2019. *Modelling and Analysis of Grid tied Solar PV System.* s.l., IEEE Transactions on Control System, pp. 66-74.

Narendra, P., Babu, P., Chittibabu, B. & Panda, G., 2019. *Three Phase Grid tied Photovoltaic System with an Adaptive Current Control Schemein Active Power Filter.* s.l., IEEE Transactions on Power Systems, pp. 19-25.

Neira, S., Linaza, A. & Pereda, J., 2020. *A Novel Three Port NPC Converter for Grid Tied Photovoltaic Systems with Integrated Battery Energy Storage.* s.l., IEEE Transactions on Power Systems, pp. 9-11.

Neira, S., Lizana, A. & Perada, J., 2020. *A Novel Three Phase NPC Convetrer for Grdi Tied Photovoltaic Systems with Integrated Battery Energy Storage.* s.l., IEEE Transactions on Power Electronics, pp. 9-13.

Noman, A., Alolah, A. & Addowesh, K., 2019. *The Three Phase Cascaded VSI Topology using coupled transformers for grid connected PV application.* s.l., IEEE Transactions on Power System, pp. 66-71.

Panday, S., 2020. *Grid Tied PV BES System with Multitasking VoltageSource Converter.* s.l., IEEE Transactions on Control System, pp. 28-36.

Pan, H., Teng, Q. & Wu, D., 2020. *MESO based robutness voltage sliding mode for AC islanded microgrid.* s.l., IEEE Transactions on Power System, pp. 30-35.

Quie, T., Liu, T., Zhang, W. & Tang, W., 2020. *Event Triggered Updating Method in Centralized and Distributed Secondary Controls for Islanded Microgrid Restoration.* s.l., IEEE Transactions on Smart Grid.

RajaMohamed, S., Aruna, P., Devaraj, D. & Bouzguenda, M., 2019. *Performance Comparison of Active and Passive LVRT strategies for Grdi Connected PV systems.* s.l., IEEE Transactions on Control System, pp. 47-53.

Rajamohamed, S., Aruna, P., Devaraj, D. & Bouzguenda, M., 2019. *Performance Comparison of Active and Passive LVRT Strategies for grid connected PV syetm.* s.l., IEEE Transactions on Power system, pp. 56-31.

Rashidi.F & Farahani.H, 2017. Direct power control of a grid-connected photovoltaic system using a fuzzy-logic based controller. *Sage Journal,* March.

Remache, S., Islam, S. & Barra, K., 2019. *Algeria Power Management of Grid Connected PV System with Integrated Energy Storage.* s.l., IEEE Transactions on Renewable Energy, pp. 11-15.

Said Romdhane.M, Naouar.M & Momasson.E, 2017. An Improved LCL filter Design in Order to Ensure stability without damping and despite large grid impedance variations, IEEE Transactions on Power Electronics.

Shi, C., Zhang, J., Zhang, X. & Liu, Y., 2020. *A New secondary reactive contro: strategy of microgrids based on droop control.* s.l., IEEE Transactions on power electronics, pp. 1-6.

Singh, B. & Tiwari, K., 2020. *CMPN Adaptive Control Algorithm for Double Stage PV Grid Connected System.* s.l., IEEE Transactions on Smart Grid.

Singh, M., Singh, O. & Kumar, A., 2019. *Renewable Energy Sources Integration in Microgrid including load patterns.* Algiers, Algeria, IEEE Transactions on power electronics, pp. 1-4.

Singh, S. & Panigrahi, K., 2020. *Enhanced Come Frequency Locked Loop based Control of Grid Tied PV System.* s.l., IEEE Transactions on Power Electronics, pp. 32-39.

Singh, S., Singh, S. & Panigrahi, K., 2019. *MRZA LMM with IMTOGI Control for Grid Tied PV system.* s.l., IEEE Transactions on Power Systems, pp. 77-81.

Soonee, K. S., Baba, K. V., Narasimhan, S. R. & Batra, P., 2019. *Renewable energy integration in India ,* Ghaziabad, India: IEEE Milan Power Tech.

Sorte, K., Panda, P. & Panda, G., 2021. *Current Reference Control Based MPPT and investigation ofPower Management Algorithm for Grid Tied Solar PV Battery System.* s.l., IEEE Transactions on Smart Grid, pp. 23-26.

Sorte, P., Panda, P. & Panda, G., 2021. Current Reference Control Base MPPT and Investigation of Power Management Algorithm fopr Grid Tied Solar PV Battery System. *IEEE System Journal,* pp. 21-34.

Suan.F, Rahim.A & Woow.P.H, 2015. Modulation Techniques to Reduce Leakage Current in Three-Phase Transformerless. *IEEE Transaction on Industrial electronics,* January.62(3).

Sun.K, Lin.X, Li.Y & Gao.Y, 2018. Improved Modulation Mechanism of Parallel-Operated T-Type Three-Level PWM Rectifiers for Neutral-Point Potential Balancing and Circulating Current Suppression. *IEEE Transaction on power electronics,* September , 33(9), pp. 7466 - 7479.

Sun, L., Wu, G., Lee, K. & Li, D., 2018. *Coordinated Control Strategy for fuel cell power plant.* s.l., IEEE Transactions on Energy Conversion, pp. 60-63.

Surendran, S., Ajayan, S. & Sruthi, S., 2017. *Advanced topology to minimize leakage current grid tied PV systems.* s.l., IEEE Transactions on Power system, pp. 7-11.

Tarek, M., Siam, A., Zia, M. & Rahman, M., 2019. *A Novel Five Level Inverter Topology with Reactive Power Control for Grid Connected System.* s.l., s.n., pp. 6-9.

Thomas, T. & Mishra, K. M., 2019. *Control Stategy for a PV Wind based standalone DC microgrid with hybrid energy storage system.* s.l., IEEE Transactions on Power Electronics, pp. 1-146.

Tiwari, K. & Singh, B., 2020. *CMPN Adaptive Control Algorithm For Double Stage PV Grid Connected System.* s.l., IEEE Transactions on Power Electronics, pp. 18-30.

Tomar, A., Mittal, N. & Sharma, S., 2018. *PV Piezo Hybrid Grid connected system.* s.l., IEEE Transactions on Smart Grid, pp. 44-51.

Venkatasamy, B., Kalaivaini, L., Prakash, P. & Prabhu, S., 2018. *Performance Analysis of Grid Tied Inverter for Reactive Power Injection Mode in Hybrid Wind Solar Energy System.* s.l., IEEE Transactions on Power Systems, pp. 9-12.

Venkatranaman, D. & John, V., 2020. *A Reconfigurable Solar Photovoltaic Grid Tied Inverter Architecture for enhanced Energy Access in Back up Power Applications.* s.l., IEEE Transactiopns on Industrial Electronics, pp. 20-24.

Wang.B, Xu.Y & Shen.Z, 2017. Current Control of Grid-Connected Inverter With LCL Filter Based on Extended-State Observer. *IEEE Transactions on industrial electronic,* July.64(7).

Wang.M, Z., 2016. *LCL filter design in T-type three-level grid-connected inverter.* Hefei,China, IEEE.

Wang, J. & Jin, C., 2018. *A uniform control strategy for the interlinking converter in the hierarchical controlled hybrid AC/DC Microgrids.* s.l., IEEE Transactions on Power Electronics, pp. 15-21.

Wang, Y. & Ren, B., 2018. *Fault Ride Through Enhancement for Grid Tied PV systems with Robust Control.* s.l., IEEE Transactions on Power Systems, pp. 19-22.

Wijesinghe, K., 2019. *Optimized Integration of Solar PV Energy on to Telecom Power Systems for DC and AC buses or Energy Storage with proposed converters to make them as profit centers.* s.l., IEEE Transactions, pp. 10-15.

Xiang, X., Ning, X., Yongyan, Z. & Wei, Z., 2018. *Study on High Voltage Grid Connected PV inverter based on Modular Multilevel Converter.* s.l., IEEE Transactions on Smart Grid, pp. 66-70.

Xiao, X., Chen, M. & Guerrero, M., 2019. *Secondary Restoration Control of Islanded Microgrids with a Decentralized Event Triggered Strategy.* s.l., IEEE Transaction on Industrial Informatics, pp. 149202-149223.

Yadzani.A, I., 2014. *Simple mathematical model of a phototvoltaic module for simulation in Matlab/Simulink.* Toronto,Canada, IEEE.

Yan, G., Hu, W., Jia, Q. & Zhang , F., 2019. *Single Stage Grid Connected Photovoltaic Generation takes part in Grid Frequency Regulation for Electromechanical Transition.* s.l., IEEE Transactions on Smart Grid, pp. 45-52.

Yan, L. & Buqiong, X., 2019. *Study on the impact of PV connection on grid on power flow based on time series output characteristics.* s.l., IEEE Transactions on Power System, pp. 67-61.

YI, W. et al., 2019. *Maximum PV Access Capacity Planning Method for Rural Power Grid considering Overload Risk.* s.l., IEEE Transactions in Smart Grid, pp. 12-19.

Yoo, H., Nguyen, T. & Kim, H., 2020. *Consensus Based Distributed Coordination Control of Hybrid AC/DC Microgrids.* s.l., IEEE Transactions on Sustainable energy, pp. 81-85.

Zarepour.E, Hassan.M & Chou.C, 2015. Performance analysis of carrier-less modulation schemes for wireless nanosensor networks. *2015 15th international conference on nanotechnology(IEEE-NANO).*

Zeb.K, Khan.I, Busarello.T.D & Ahmad.I, 2018. Review on Recent Advances and Future Trends of Transformerless Inverter Structures for Single-Phase Grid-Connected Photovoltaic Systems. *Energies 2018,* 11(8).

Zeb, K. et al., 2019. *DC Link Voltage Regulation of Single Phaser Grid Tied PV System using Fuzzy PI Controller.* s.l., IEEE Transactions on Power Systems, pp. 5-9.

Zhang, L., Qin, J., Shi, D. & Wang, Z., 2018. *Design and Performance Evaluation of the Modular Multilevel Converter based Grid Tied PV Battery Conversion System.* s.l., IEEE Transactions on Power System, pp. 15-23.

Zhao.N, W., Huo.J, Xu.D & Zhu.L, 2018. Inverter Power Control Based on DC-Link Voltage Regulation for IPMSM Drives Without Electrolytic Capacitors. *IEEE Transactions on Power Electronic,* Junuary, 33(1), pp. 558 - 571.

Zhou, N., Zhao, R., Wang, L. & Zhang, P., 2020. *A Predictive Deadbeat Grid Connected Control Method of H6 Topology.* s.l., IEEE Transactions on Smart Grid, pp. 36-41.

Zhu, Y., Xiao, Y. & Zhong, L., 2019. *Voltage Segment Coordinated Control Strategy for Isolated DC Microgrid with Multiple Energy Storage Units.* s.l., IEEE Transaxctions on Power Electronics, pp. 2204-2213.